Project no. 265432

EveryAware

Enhance Environmental Awareness through Social Information Technologies

http://www.everyaware.eu

Seventh Framework Programme (FP7)

Future and Emerging Technologies of the Information Communication Technologies (ICT FET Open)

D4.1: Report on data coverage and interpolation methods

Period covered: from 01/03/2011 to 31/08/2012
Start date of project: March 1st, 2011
Due date of deliverable: Aug 31st, 2012
Distribution: Public

Date of preparation: 31/08/2012
Duration: 36 months
Actual submission date: Aug 31st, 2012
Status: Final

Project coordinator: Vittorio Loreto
Project coordinator organisation name: Fondazione ISI, Turin, Italy (ISI)
Lead contractor for this deliverable: Vlaamse Instelling voor Technologisch Onderzoek N.V. (VITO)

Executive Summary

The EveryAware platform, cosisting of a SensorBox, a smartphone and the backend system, which is decribed in detail in Deliverable 1.1, supplies information on noise and air quality to the user community. The main aim of this document is to investigate how the EveryAware platform should be used in order to fulfill data coverage requirements for specific tasks in a scientifically sound way. To do so, one should take the highly dynamic behaviour, both in space and time (i.e. spatio-temporal variability), of noise and air quality in urban environments into account. Both noise and air quality are locally influenced by the emission sources. In contrast to noise, which dies out almost instantaneously after the source stops producing it, air pollutants stay in the atmosphere for longer periods, yet they get diluted, transported and transformated. The location and time of measurement is thus heavily determined by the local circumstances at that specific point in space and time. One measurement at that location thus provides a spatio-temporal snap-shot, which is not necesserily representative for a longer period or greater area.

The specific tasks where the EveryAware platform is used for by the user community are event-based measurements, the mapping of the local noise and air quality or exposure monitoring to these pollutants. Based on several Pilot Cases and Beta Test Cases (which are further discussed in Deliverables D3.1 and D6.2) the data coverage requirements to satisfy the specific measurement goals were investigated for air quality and noise. Key results from this assessment for air quality were:

- **Repeated measurements** are crucial to get a representative figure of the air quality. **Mobile collection** of data is the most suitable data collection method to obtain repeated measurements, covering a much larger area than would be obtained by stationary measurements with the same number of SensorBoxes.
- To draw broad scale pollution maps street level **aggregation** is a first useful and in many cases sufficient step. This levels out part of the variability that is related to traffic discontinuity and short-term incidents, but might underestimate intra-street variability.
- Taking into account the large data needs to get a representative picture of urban air quality and the fact that, both because of its cost and its technical complexity, the SensorBoxes will be distributed to a rather limited group of people (as opposed to the Widenoise app), data collection should **focus** on a clearly defined time frame and area in order to obtain sufficiently repeated air quality measurements. This calls for a **targeted data collection** approach.

Noise measurements is not confined by additional harware needs such as a SensorBox for air quality measurements and could be made by the entire EveryAware user community. However, the results of the Beta Test Cases and Pilot Cases demonstrate that uncoordinated sensing across a large area does not lead to dense spatial and temporal coverage. Reaching dense coverage without coordination would require massively more contributors, which may not be attainable in the short term. An alternative approach is to foster collaboration between smaller groups of highly motivated contributors that live close to one another. By coordinating the actions of such groups it is possible to achieve dense spatio-temporal coverage, albeit for much smaller areas. The key

findings for data coverage with respect to noise measurements is to move towards a more **coordinated**, **goal-driven** approach by devising **targetted data collection** protocols.

In addition to the EveryAware measurements, interpolation methods could potentially estimate air quality and noise at points in space or time where measurements are lacking. The second aim of this report is to assess the potential of interpolation methods to increase the EveryAwere data coverage. The key finding of this assessment was that due to the central shared assumption of a continuous surface generic interpolations methods are not that suitable for interpolation urban noise across large areas, due to the limited spatial and temporal reach and the effect of obstacles such as buildings. Also the highly dynamic behaviour of air pollutants in an urban environment and the fact that the urban outdoor environment largely consists of discontinuous line elements, interferes with the application of the described interpolation methods. Studies in which interpolation methods were used for air quality are generally conducted on a much lower resolution (e.g. yearly averages, 5 km by 5 km grids) than what would be suitable for EveryAware.

Contents

List of Figures

Chapter 1

Overview

This document gives a description of a part of the work that has been carried out in the WP4 of the EveryAware project. The final objective of this document is to derive a list of recommendations on data collection and data handling so that a sufficient data coverage during the deployment of the EveryAware case studies is reached.

To reach this goal, the spatio-temporal characteristics and data coverage of air quality and noise in urban environments was investigated based on literature review and several pilot cases. The assessment is subdivided in different sections. Firstly, a methodological framework is defined by which data coverage in EveryAware is discussed. Its relation to the measurement goals and data collection schemes is established. Data coverage for air quality monitoring is discussed in a second section. Air quality is spatially and temporally very heterogeneous, exhibiting high gradients over short periods or distances. Data coverage for air quality monitoring is assessed with this highly variable background in mind based on a literature review and three pilot cases. Conclusions from this section for the development of the EveryAware Test Cases for air quality monitoring are drawn. The final section of the data coverage assessment concerns noise. Within the context of the EveryAware project we focus exclusively on the problem of environmental noise. Environmental noise is the noise people are exposed to in their daily lives as a result of various human activities, such as those related to transport, industry and leisure. Several campaigns have been set up using WideNoise to measure noise in a daily environment. Each of these campaigns had specific goals. The data coverage of the campaigns is discussed in this documents. The data coverage statistics that characterize these campaigns are highlighted, and can assist in estimating data coverage of the test cases through extrapolation.

The revision and use of interpolation methods has been carried out. An overview of the most commonly applied interpolation models in environmental sciences is providedand their potential of application in EveryAware has been assessed.

Chapter 2

Data coverage

2.1 Introduction

2.1.1 Definitions

In EveryAware, data **coverage** is defined in two domains: (1) temporal coverage and (2) spatial coverage. Coverage is a relative concept. Temporal and spatial data coverage is called sufficient if the underlying physical reality is adequately described. This depends on the goals for which data are collected, and on the spatial and temporal variability of the feature that is measured (e.g. air quality at a specific location). As such coverage is intrinsically linked to representativeness.

For instance, a certain area can be properly spatially covered but only for one point in time for each year. In this case temporal coverage is poor if the underlying variability during the year is high and we want to draw conclusions on a broad time frame. However, if the underlying physical reality, e.g. the spatial co-ordinates of a road, do not vary very much in time, temporal coverage is sufficient.

Data coverage is directly linked with the information requirements to serve the data collection goals. A spatio-temporal snap-shot of air quality or noise can be obtained by one measurement at a given location in space and time. In order to get a representative estimate of air quality or noise level at a given location, however, data collection should be increased to deal with the temporal dynamics of the pollutants. Urban air quality as well as urban soundscapes are highly dynamic and the air quality or sound level that is measured or heard at a certain moment and/or location is not necessarily representative for that time or place.

In addition to the temporal and spatial coverage, the temporal and spatial **granularity** is another integral feature of the spatio-temporal sensor data of EveryAware. It reflects the level of detail, both in time and space, by which an event is characterized. It is the level of detail at which events are captured in dimensions (space, time). Granularity also relates to the fact that the space-time frame associated to an event of interest can be envisaged at several levels of detail (e.g. hour, day, month, street, urban, etc.).

The detail discernible in the EveryAware database depends on the temporal and spatial **resolution** of the sensor and refers to the size of the smallest possible events that can be detected. Theoretically, very short (temporal resolution of the sensor) and localized (spatial resolution of the GPS) events could be discernible from the point data of the EveryAware database. Temporal resolution is 5 to 15 seconds in case of a WideNoise data entry and one second in case of a single air quality measurement with the EveryAware SensorBox. Spatial resolution depends on the distance that the sensor has travelled in that time, and on the spatial accuracy of the GPS.

Finally, although a single sensor datum has a very narrow spatial resolution, the measurement itself may be influenced by distant sources. Noise or air quality measurements may be influenced by sources at a few to hundreds of meters, depending on e.g. the noise or air pollution source characteristics, pollutant dynamics, atmospheric residence times and meteorological conditions.

As data coverage requirements depend on the different goals to which the EveryAware sensor measurements can serve, these are described in more detail in section 2.1.2. Spatio-temporal variability of air quality and noise is described further in 2.2 and in 2.3.

2.1.2 Goals of data collection

The reasons for volunteers to collect data within the EveryAware framework can be manifold. Nevertheless, we assume that a significant part of the collected data will be used for the following three data collection goals: (1) event-based measurements, (2) mapping of an area or (3) personal exposure assessment.

Event-based measurements

EveryAware measurements are used to quantify a characteristic of an event. We define an event as something happening, i.e. a discontinuity, that is clearly distinguishable from the normal spatio-temporal pattern and clearly confined in space and time. An event is related to a specific source that causes pollution or noise. An event-based measurement tries to capture the impact of an event both in space or in time. Examples are a noise measurement during a concert or an air quality measurement during roadworks. Of course, the sound level (as well as other acoustic parameters) and the perception thereof varies a great deal over the course of the event and depending on where in the venue the measuring device or the listener is positioned. Similarly, the emission of air pollutants and resulting local air quality varies greatly during the roadworks. Events can also be recurrent, e.g. a plane flying over every day. This adds still another source of temporal and spatial variability.

For the detection of events (noise event, pollution event) individual point data are not very useful because the lack of background measurements (i.e. measurements during the normal situation, just before and after a particular event). In this sense, series of data (time series at one location or space-time series of measurements collected in a mobile way) are far more informative. Time series of noise or air quality data will exhibit peaks at occasions of significant difference with current background conditions, and are therefore suitable to identify events in time. Spaio-temporal series acquired by measurements at a fixed time interval along a certain route are suitable to identify exceptional spatio-temporal events such as air pollution hotspots at congested roads during the morning rush.

Mapping the (local) area

EveryAware measurements are used to map air quality and noise in a given area. A map can be used to display point measurements. However, these are merely snapshots of the situation at a specific moment in time with little broader relevance. To be useful for personal or community decision making, maps need to give a more representative picture by data aggregation over relevant time frames and locations. The spatial and temporal coverage needs to be sufficiently high to allow for this aggregation. Temporal coverage needs to be in line with the time period for which the map is valid (e.g. average pollution during morning peak hours on weekdays in September).

Personal exposure

EveryAware measurements are used to compute personal exposure to air pollution or noise during a specific time frame. When repeated, these personal exposure data can give rise to more generalised personal exposure patterns which can be used for optimising personal choices or community choices.

2.1.3 Data collection schemes

EveryAware measurements basically all have the same data structure. Each measurement is characterized by time, location, parameter value and subjective annotation or tag. As such a spatio-temporal dataset (E) is acquired. $E = \{\mathbf{x}_1, \mathbf{x}_2, \cdots, \mathbf{x}_n\}$ where $\mathbf{x}_i$ = (time$_i$, location$_i$, measurement$_i$, annotation$_i$, tag$_i$). Nevertheless, data collection modes may be very different. An overview of the most commonly used data collection modes is given below. The data collection modes are assessed on temporal and spatial coverage, planning, effort and commitment of the users.

Targeted versus opportunistic data collection

In a **targeted** data collection scheme, volunteers deliberately plan and carry out measurements with a specific purpose in mind. They concentrate efforts in a specific area over a specific time frame in an attempt to get a representative picture of reality. In an **opportunistic** data collection scheme, on the contrary, measurements are collected by volunteers in their normal daily routines. The participant does not decide on measurement location and time from his/her interest to monitor a given event. They do not envisage to cover a specific period of time, nor a specific location or route. Opportunistic data collection (ideally) requires measurement devices that measure continuously without any intervention of the user. It will result in a (possibly) sparse dataset of sensor recordings at minimal planning, efforts and commitment for the user.

Stationary versus mobile data collection

Stationary or fixed data collection refers to a collection scheme in which measurements are made at one specific location over a well-defined time window (time series of data) with a measurement instrument fixed on a wall or a pole without permanent supervision or presence of a volunteer. Stationary data collection is typically carried out in a targeted fashion, by one individual or by a group of people. The spatial coverage may range from one specific location to the coverage of a spatial grid. As such, the temporal dynamics of a parameter are measured in a spatially explicit fashion. The temporal data coverage is high. Spatial coverage depends on the number of deployed measurement devices in comparison to the extent of the area that is monitored, but is –at least for air quality monitoring– still rather high compared to classical networks of monitoring stations. The planning, efforts and commitment for targeted stationary data collection are moderate.

Mobile data collection refers to the collection of data along a route. For example, a volunteer performing measurements while commuting to and from his work is performing a mobile data collection. As such systematic spatio-temporal datasets from a route (e.g. a couple of streets) over a well-defined time frame (e.g. during the morning peak hours) are acquired. Mobile data acquisition can be performed in targeted or opportunistic (random) fashion.

- Targeted mobile data collection is performed by volunteers carrying out systematic mobile measurements in a well-defined area (e.g. a couple of streets) and time frame (e.g. during the morning peak hours). The planning, efforts and commitment for this type of measurements is high, but this type of data collection can result in a high spatial and temporal coverage. Alternatively targeted mobile data collection can also envisage the collection of systematic personal exposure data sets.

- Opportunistic mobile data collection along random routes is performed by volunteers who collect sensor data along their route, where-ever they go. Although these measurements were not actively planned by the user's community, they are useful for mapping and exposure calculations. The planning, efforts and commitment for this type of data collection should be

relatively low, but depends on user friendliness of devices, i.e. the capability for continuous measurements without intervention of the user. The data coverage depends on the variability (space, time) and repetition of the routes taken by the volunteers, and the time spent outdoor.

Semi-stationary data collection refers to the collection of data for a limited period of time (e.g. one hour) at a fixed location by a volunteer carrying the measurement device. In practice data collection with portable measurement devices can lead to a mix of mobile and semi-stationary data, both in targeted data collection schemes as in opportunistic data collection schemes, e.g. when a volunteer waits for a bus for ten minutes or when he attends an outdoor festival for 3 hours.

2.2 Air quality monitoring

The assessment of data coverage for air quality monitoring is based on insights from three targeted measurement campaigns: (1) a measurement campaign carried out in the CLIMAQS and IDEA projects (funded by the Flemish Agency for Innovation by Science and Technology) - this data set can be thought of as an opportunistic data set, i.e. covering same route but not systematically in time, (2) a recent systematic mobile measurement campaign carried out in Antwerp with targeted mobile data collection, and (3) a pilot case study in Antwerp conducted during the EveryAware partner meeting in Antwerp (July 9-10, 2012).

The EveryAware SensorBox was not used in any of the campaigns here. However, all the three campaigns focussed on traffic related pollutants (UFP, PM10 and BC) in urban areas. SensorBox data are most likely to behave similar to these parameters. Therefore, insights and conclusions from these campaigns are valuable for the set-up of the case studies in EveryAware. Additionally, the EveryAware SensorBox will be calibrated against the high quality device used in the second monitoring campaign (BC micro-aethalometer). The use of the SensorBox also shows parallels with the sensors used in the pilot cases. The use of the SensorBox –and other air quality measurement devices– is much more complicated than for example the use of the WideNoise app for noise. Air quality devices need (repeated) calibration (see D1.1), they need a methodical operation with and are thus not suited for opportunistic data collection. Data collection of the pilot campaigns used a targeted mobile data collection, which is also the appropriate data collection method using the SensorBox.

2.2.1 Urban air quality

The urban air contains a complex mixture of potentially noxious components such as nitrogen oxides (NOx), carbon monoxide (CO), ozone (O_3), volatile organic compounds (VOC) and particles of mixed composition, ranging in size from a few nanometer to several micrometer. For most pollutants urban concentrations are composed of a regional background with on top of it a more elevated urban background, and finally a source dependent local contribution, as described initially for PM10 in [Lenschow et al., 2001]. The local air quality component in urban areas varies highly both in space and time. It is highly related to traffic, and thus to local variability in traffic. It is further strongly affected by local street lay-out and meteorological circumstances, which affect dispersion, and short-term chemical and physical transformations (e.g. oxidation of NO to NO_2, condensation and coagulation of particles, etc.)[Nikolova et al., 2011]. It contributes disproportionally to human exposure to air pollutants, as these pollutants are emitted near nose height and in close proximity to people [Dons et al., 2011, 2012; World Health Organization, 2000].

The best indicators of the presence of traffic pollution are those air pollution components that leave the vehicle tail pipes in a relative large amount compared to the concentrations already present in the urban background, and for which no other major sources are present in the urban atmosphere. Nitrogen oxides (NOx), Ultra Fine Particles (UFP), Black Carbon (BC) and the smallest fraction of

fine dust (PM1) are known to comply very well to this requirement (e.g. [Dons et al., 2011]). All of these components are to a certain extent correlated to each other, but they all have their own dynamics. This is described in more detail for particles in next paragraph.

2.2.2 Spatial and temporal variability of urban air quality: short literature review

Particulate air pollution is a mixture of particles that vary in number, size, shape, surface area, chemical composition, solubility and origin, where the size distribution is typically trimodal, including coarse particles (aerodynamic diameter > 2.5 μm), fine particles (aerodynamic diameter between 0.1 and 2.5 μm) and ultra-fine particles (UFP, aerodynamic diameter < 0.1 μm) [Pope III and Dockery, 2006]. PM10 is primarily derived from suspension and re-suspension of solid material, and contributes greatly to the mass of the total suspended particles in urban environments. In contrast, UFP contribute little to the mass of the total suspended particles but they are highly abundant. The urban particulate cloud is constantly receiving UFP from primary emissions from combustion sources in transportation, industries and power generation, and by secondary formation by atmospheric photochemical reactions and conversion processes [Seinfeld and Pandis, 2006; Westerdahl et al., 2005]. UFPs have a transient nature with short life times (minutes to hours) and rapidly grow through atmospheric processes of coagulation and/or condensation to larger complex aggregates [Pope III and Dockery, 2006]. Therefore, the highest concentrations of ultra-fine particles are found in the vicinity of the primary sources, for example, near busy roads where particle number concentrations are typically between 10^4 and 10^6 particles cm^{-3} depending on driving speed, fleet composition and meteorology [Nikolova et al., 2011] and ultra-fine particle number concentrations decrease rapidly with distance from the emission sources [Hagler et al., 2010; Zhu et al., 2002]. Therefore important differences, in space and time, of UFP concentrations between urban micro-environments are induced [Hudda et al., 2010].

Small-scale variations in PM10 concentrations have also been reported elaborately in the literature. Temporal patterns of PM10 have been observed over seasons [Monn et al., 1997], weeks [Monkkonen et al., 2004], days [Roosli et al., 2000] and hours of the day [Gomiscek et al., 2004] in urban settings and were attributed to the temporal dynamics of atmospheric conditions and the PM10 sources. The spatial variability of PM10 within the urban environment differs in the literature from rather limited [Roosli et al., 2000] to substantial [Chan et al., 2001; Wilson et al., 2006], which may be predominantly caused by the spatial heterogeneity of the main sources.

The soot-black carbon (BC) component of the urban fine particle cloud has been associated with adverse health effects (e.g. [Brugge et al., 2007]). From a study in Helsinki, it was shown that typically more than 90% of BC resided in the PM2.5 fraction [Viidanoja et al., 2002]. A major source of BC in urban areas is direct combustion (especially from diesel combustion). BC shows a high spatial variability, and high contrasts between busy streets and background locations in the same city were found for BC [Boogaard et al., 2011]. The high spatial variability of BC is also reported in other studies [Wang et al., 2011] which found a high spatial divergence in BC between several monitoring sites in Rochester, New York. Also for BC a high temporal variation has been observed (daily and seasonal trends, [Latha and Badarinath, 2005]). The high spatial and temporal variability of BC concentrations in relation to the time-activity pattern of people results in different exposure patterns [Dons et al., 2011, 2012].

We used three data sets from mobile monitoring campaigns to investigate to what extent a limited set of mobile measurements spread over different days and different times of the day allows to draw conclusions on spatio-temporal variation in urban air pollution and to map urban air quality for different data collection goals. The first and second data sets were collected by VITO in measurement campaigns that were part of the IDEA project (funded by the Flemish Agency for Innovation by Research and Technology). The third data set was collected specifically for EveryAware. The first campaign focussed on UFP and PM10, the second and third campaign focussed on BC.

Table 2.1: Overview of some street characteristics at a selection of streets along the mobile monitoring routes in Antwerp and Mol.

	Street name	Speed limit	Configuration	Traffic density [day-1]*		
				light	heavy	total
Antwerp	Bleekhofstraat	50 km h-1, 30 km h-1	1 lane	4 074	8	4 082
	Provinciestraat	50 km h-1	1 lane, street canyon	13 495	4	13 499
	Carnotstraat	50 km h-1	1 lane, street canyon, separate biking lane	21 396	119	22 515
	Plantin en Moretuslei	70 km h-1	2 lanes, separate biking lane	42 961	420	43 381
Mol	Turnhoutsebaan	70/50 km h-1	1 lane, separate biking lane, commercial and residential	9419	297	9716
	Statiestraat	50 km h-1	1 lane, street canyon, residential and commercial	4143	262	4405
	Rozenberg	50 km h-1	1 lane, separate biking lane, residential	5603	115	5718
	Kleinendijk	50 km h-1	1 lane, green (recreational) zone	NA	NA	NA
	Gasstraat	50 km h-1	1 lane, residential	1852	0	1852
	Voogdijstraat	50 km h-1	1 lane, street canyon	6023	326	6349

*Data source: Traffic Centre Flanders.

2.2.3 Air quality case study: PM10 and UFP

Study site Mobile measurements were performed at two locations, Antwerp (51°12'N, 4°26'E) and Mol (51°11'N, 5°07'E), Belgium. Antwerp is a medium-sized city (480 000 inhabitants, 985 inhabitants km^{-2}), Mol is a provincial town (34 000 inhabitants, 299 inhabitants km^{-2}). At both locations, a fixed route was defined using cycling paths or the right side of the road. The route in Antwerp was approximately 5 km long, the route in Mol 10 km. Average travelling time for the entire route were approximately 25 minutes for Antwerp and 50 minutes for Mol. Although the major part of the mobile routes were located in residential area, streets of differing configuration and with differing traffic dynamics were included in this study. The results presented in this study are focussed upon a selection of six streets in Antwerp and Mol which reflect the variation in traffic density, driving speed and street configuration (Table 2.1). Additionally, a recreational area with very low traffic density was included along the route in Mol. After a data quality control, 24 runs on 8 days in the period between March 16 and April 8, 2009 were withheld in Antwerp. In Mol a total of 20 runs were performed on 10 measurement days between April 7 and April 23, 2010. The monitoring hours ranged from 6 am until 6 pm, but most of the runs were made between 10 am and 4 pm. The repetition frequency of the measurement runs (number of runs per day, time of the day) was partially determined by practical and organizational circumstances. This led to a non-uniform distribution of the measurements over the day. All measurements were carried out during working days.

Mobile platform Portable UFP and PM monitors were installed on a bicycle (the so-called Aeroflex, Fig. 2.1) which was additionally equipped with a GPS (Garmin Forerunner) to register measurement location and a smartphone (Openmoko FreeRunner) to synchronize the sensors and to communicate the data to the central database. A TSI P-Trak ultra-fine particle counter (model number 8525) was used to measure the number concentration of ultrafine particles within a range from 0 to $5 \cdot 10^5$ particles cm^{-3} at a temporal resolution of 1 sec. A DustTrak DRX 8534 was used in Antwerp for measuring PM10 mass concentration (μg m-3), whereas in Mol the PM10 concentration was measured by a GRIMM 1.108 Dust monitor. The instruments were recently calibrated and operated at flow rates of 1.7 L min^{-1} and 1.2 L min^{-1}, respectively. The outdoor temperature was within the operating temperature range. PM10 concentrations were measured at a 1 and 6 second resolution in Antwerp and Mol, respectively. A similar mobile platform set up as the mobile set up for Mol was shown to have a robust performance in a similar urban environment [Berghmans et al., 2009].

Analyses An analysis of the temporal and spatial variability of the air quality measurements was conducted to assess the potential of using mobile measurements to distinguish between episodes of low or high particle concentrations, and between locations (streets) of contrasting particle concentrations. A post-hoc multiple comparison between measurement days, time of the day, or street

Figure 2.1: The Aeroflex measurement bike from VITO.

was performed using the results of a Kruskal-Wallis test with a Bonferroni adjustment of the critical value to compensate for multiple comparison. Given the relative nature of the spatio-temporal assessment, errors due to instrumentation differences (e.g. DustTrak DRX 8534 vs. GRIMM 1.108) and differences in meteorological conditions were reduced.

Given the spatio-temporal dynamics of the pollutants under investigation and the fact that mobile measurements provide snap-shots of pollutant concentrations in space and time, an experiment was conducted on the data to investigate data coverage in relation to data representativeness. The research question addressed was how many mobile runs are needed to obtain a representative estimation of the street-level air pollution. In this study, representative means that the estimation is reasonably similar (max. 15% difference) to the value obtained from the entire mobile measurement campaign. Additionally, we assessed how sensitive the results are for the timing of those runs.

First, all the data were used to calculate an aggregated median pollutant concentration per street over all the measurement runs. We preferred to use the median concentration because air quality measurements are not normally distributed and skewed, so the median is a more representative central tendency measure than the mean. Subsequently, median pollutant concentrations were calculated per street based on mobile measurements of a cumulatively growing data volume that was obtained by a cumulative addition of measurement data from randomly selected runs (random selection without replacement). The median pollution concentrations in function of the increasing number of runs were compared to the overall median value to see after how many sampled runs the medians converged to the overall median. Convergence is obtained when the median of the sampled runs deviates less than 15% from the overall median, and does so consistently when adding new runs. The pseudo-code for this experiment is given below. The pseudo-code was run a high number of times (10 000 iterations) to guarantee a high number of possible combinations of runs. The number of runs needed for convergence for each combination of randomly selected runs was plotted in a density plot.

Results A clear distinction is observed between the spatio-temporal dynamics of UFP and PM10, respectively (Fig. 2.2). UFP showed a high variability in space (between streets) and time (between measurement runs). The temporal changes of UFP concentration in Antwerp and Mol were present in both busy and quiet streets. High spatial differences between streets were also observed, with high concentrations for Provinciestraat in Antwerp and for Voogdijstraat in Mol. Other streets consistently showed lower UFP concentrations. In contrast to the spatio-temporal pattern

Algorithm 1 Pseudo-code to determine the number of runs needed for convergence

Require: Mobile measurements made during k runs along the same route of UFP and PM10
  randomly permute the k runs;
  calculate overall median UFP and overall median PM10;
  for $i = 1$ to k **do**
    select pollutant data from the i first permuted runs;
    calculate the median UFP and median PM10 concentration, save;
    calculate the difference of median UFP and median PM10 with overall median UFP and overall median PM10, respectively (as %), save;
  end for
  identify the number of runs at convergence; save

of UFP, PM10 showed a quite different pattern. The variability in space for PM10 was very limited compared to the variability in time. The PM10 concentrations did not differ a lot between streets. The variability in time was high between runs carried out on different measurement days, but much lower between runs carried out at different hours within the same measurement day.

A statistical analysis of the spatial pattern of UFP and PM10 concentrations revealed significant concentration differences between the streets of the route in Antwerp and Mol (Fig. 2.3, Chi-sq. = 2711, p < 0.01). The highest UFP concentrations were measured in Carnotstraat and Provinciestraat, followed by Kroonstraat, which were significantly higher than the UFP concentrations in Plantin en Moretuslei and Bleekhofstraat. The lowest UFP concentrations were found in Langstraat. In Mol, significantly different UFP concentrations were also found between several streets (Fig. 2.3, Chi-sq. = 9766, p < 0.01). The UFP concentration in Voogdijstraat was significantly higher than in all the other streets along the route, whereas the concentrations at Kleinendijk were significantly lower than in the other streets. Between both extremes, Voogdijstraat and Kleinendijk, several other streets differed significantly in UFP concentration.

The spatial variability of PM10 was lower, but overall significant in Antwerp (Chi-sq. = 626, p < 0.01) and Mol (Chi-sq. = 46, p < 0.01). In Antwerp, measured PM10 concentrations were significantly higher in Carnotstraat in comparison to Provinciestraat and Kroonstraat, where the PM10 concentration was significantly higher than in all the other streets along the route (not shown). The PM10 concentration in these streets, however, were not significantly different. The differences in PM10 concentrations between streets in Mol were overall significant, but the multiple comparison test revealed that the this significance was solely attributed to the difference in the PM10 concentration at Gasstraat which was significantly lower than in Statiestraat and Rozenberg. The streetwise comparison did not reveal any other significant difference.

Experiment: How many runs are needed? One experiment was conducted (see Alg. 1), by which mobile runs were randomly and cumulatively added to calculate median street UFP and PM10 concentrations from a cumulatively growing dataset of mobile measurements. The data set is quite sparse, and the time intervals for the mobile runs were different on every day. In Antwerp, the total daytime interval in which mobile runs were carried out, was from 6 am until 6 pm. However, for many hours of the day only one or two runs were available. In Mol, measurements were performed on a daytime interval from 11 am until 3 pm.

Results indicated differences between UFP and PM10 at both study sites (Fig. 2.4). For the analysis of the UFP data set, the maximal number of runs required for UFP for convergence was 18 (out of 24) for Antwerp and 16 (out of 20) for Mol. At both measurement locations, however, 75% of the combinations convergence was already reached with a number of runs that was approximately 70% lower (7-8 instead of 24 runs in Antwerp, 6-7 instead of 20 runs in Mol). Inspection of the results for the individual streets showed differences between the streets. In Antwerp, an early

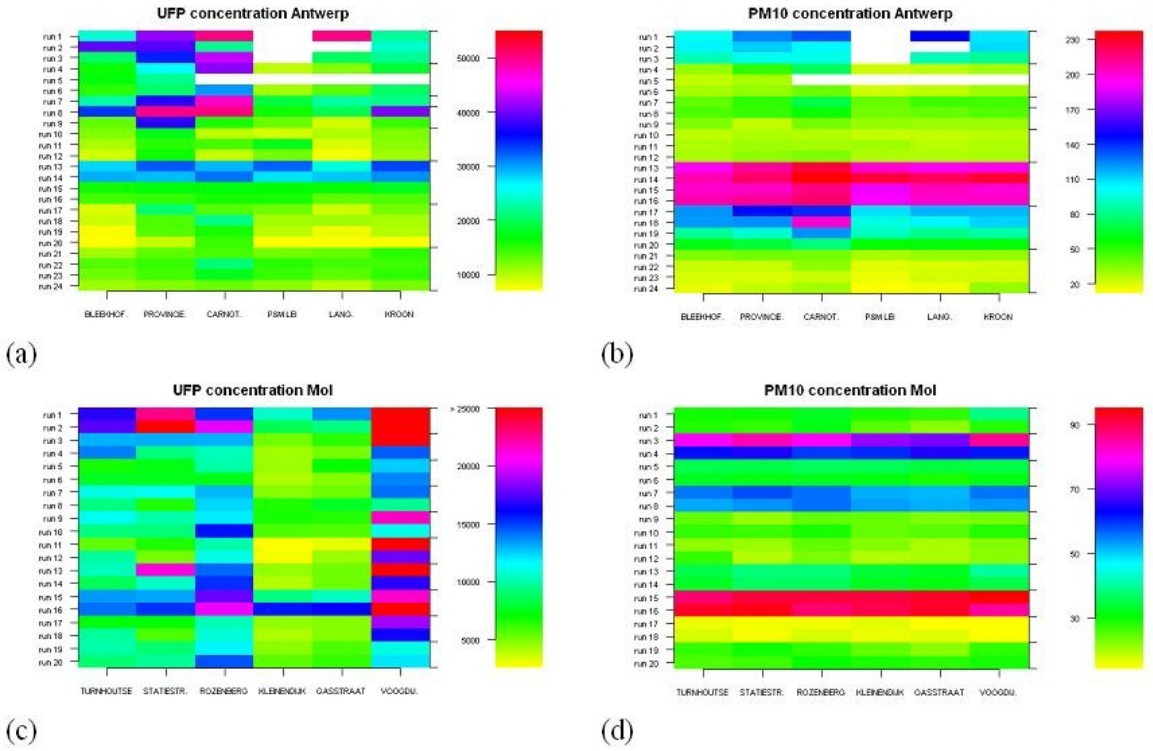

Figure 2.2: Median UFP and PM10 concentrations for the different runs (y-axis) at a selection of streets (x-axis) in Antwerp and Mol. The different measurement days are indicated by the ticks on the second y-axis. The colours are scaled between the extremes and differ between the plots. White pixels represent no data.

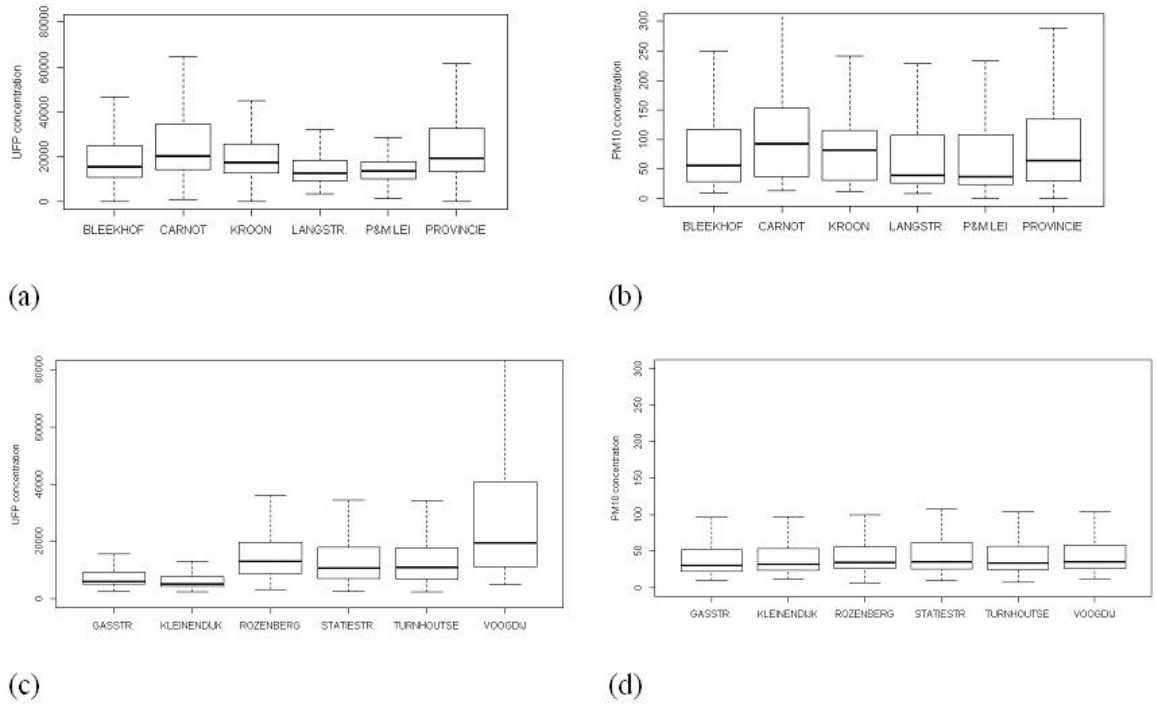

Figure 2.3: Boxplots of UFP concentration in Antwerp (a) and Mol (b) and boxplots of PM10 concentration in Antwerp (c) and Mol (d) for a selection of streets.

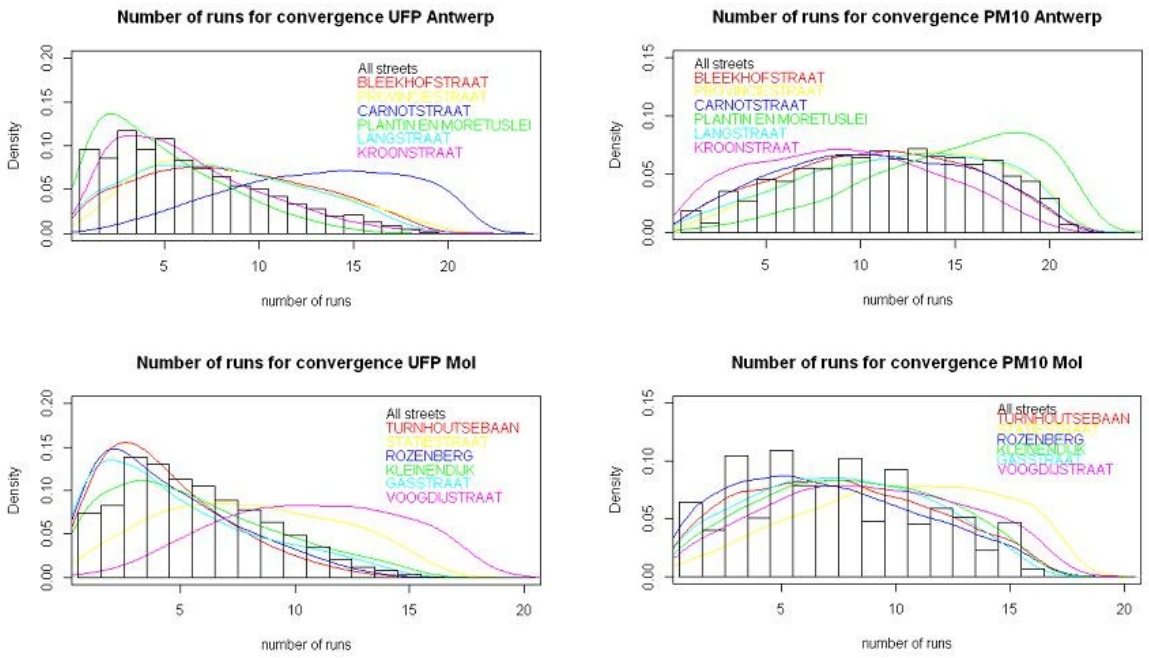

Figure 2.4: Plots of the number of runs needed for converge of the median concentration for UFP and PM10 at the study sites of Antwerp and Mol. The histogram plot shows the number of runs needed for convergence based on all the measurements, the coloured density plots show the results for specific streets.

peak around 2-3 runs was observed in the density curve for Plantin en Moretuslei and Kroonstraat, whereas this peak was shifted toward a higher number of runs (5 to 8) for Bleekhofstraat, Provinciestraat and Langstraat, and a much higher value (15) for Carnotstraat. For Mol, most streets showed a similar curve, except for Statiestraat and Voogdijstraat where the UFP measurements only converged after a higher number of repeated measurement runs.

The differences between Antwerp and Mol were higher for PM10 than for UFP, yet a higher number of repeated measurement runs were required at both locations. The maximum number of runs needed for convergence reached values of 20 and 15 for Antwerp and Mol, respectively. 75% of the combinations of runs reached convergence after 14 and 9 runs, respectively, which is a reduction of the total number of runs by 40 to 55%. In general, convergence was observed after a lower number of measurement runs for UFP than for PM10. The density plots of the different streets at both study areas was not very different for most of the streets. Only Plantin en Moretuslei in Antwerp generally needed a higher number of repeated runs and Kroonstraat a lower number of runs in comparison to the other streets along the route. In Mol, Statiestraat needed a higher number, and Rozenberg a lower number of repeated runs.

Discussion and Conclusion Small-scale spatio-temporal gradients in particle concentrations are already well described in the literature (e.g. Monn, 2001, and reference therein). They are caused by the spatio-temporal variability of a multiplicity of sources, dispersion and removal mechanisms. In an urban area, motor vehicle emissions usually constitute the most significant source for UFP. Typical background concentrations are far below the urban UFP concentration, and have a very small contribution to the urban UFP concentration [Nikolova et al., 2011]. The location and lay-out of roads and the dynamics of the traffic (volumes, speed, fleet composition) are the main factors affecting the spatio-temporal heterogeneity of the UFP concentration. Furthermore, atmospheric dispersion, particle coagulation and particle deposition mechanisms are also influenced by building density, by the geometry of the street and the urban canopy and by meteorology there-

fore attributing to the spatio-temporal variability of UFP number concentrations. Our measurement results are consistent with these findings in the literature. For UFP significant differences were found between measurement days and between runs on the same day (Fig. 2.2). It is well known that important diurnal changes occur in UFP concentrations due to changing traffic and other local sources throughout the day and these source variations are likely to cause the temporal UFP variations in our study as well.

[Lenschow et al., 2001] identified long range transport, motor vehicle exhaust and tyre abrasion and resuspension of soil particles as the major PM10 sources in urban areas. All these components have their own spatio-temporal dynamics. The contribution of urban background to the PM10 at the road, which was observed to be around 60% in Berlin [Lenschow et al., 2001] is more important than the background component in UFP measurements at the roadside due to the short atmospheric residence time of the latter. Our measurements indicate that for PM10 the differences between the days are more pronounced whereas intraday variation is often non-significant. The latter does not mean that intraday variability of PM10 on these days was non-existent, but may be explained by the importance of the background contribution which masks the short-term local variability of PM10. Overall, we found a higher small-scale spatial variation for UFP than for PM10.

To allow for a systematic comparison between different locations all data were aggregated at street level. This streetwise comparison shows significant differences for UFP between streets both in Antwerp and in Mol. For PM10 the spatial variability is lower. In Mol streets with higher traffic volumes could clearly be distinguished from more quiet back-end streets. This is less apparent in Antwerp, where UFP concentrations in the street with the highest traffic volume (Plantin en Moretuslei) were surprisingly comparable to the streets with the lowest traffic volume (Langstraat), and significantly lower than streets with intermediate traffic volumes (Carnotstraat and Provinciestraat). This is caused by the street lay-out with a separate biking lane at several metres distance from the traffic lanes and rather smooth traffic, whereas in Carnotstraat and Provinciestraat cyclists ride right next to or even in the wake of the cars and traffic gets easily congested. The street-level aggregation does not take into account intra-street variability. On the other hand this allows to level out part of the variability that is related to traffic discontinuity and short-term incidents. We assume most streets that were included in the measurement campaigns, to be discontinuous line sources with rather homogeneous lay-out.

Data from runs on different days and on different moments of the day are aggregated. A potential source of bias in this streetwise comparison is the fact that diurnal traffic patterns might be different between streets, and that sampling could mainly have taken place at moments corresponding to high traffic in one street (e.g. end of school) and simultaneous low traffic in other streets (e.g. not affected by school traffic). Both issues can be tackled by increasing data coverage by increasing the number of runs. This would allow to aggregate the data at a more detailed level, i.e. distinguishing non-homogeneous street sections and intersections, and aggregating data in relevant time intervals, e.g. hourly averages, peak and off-peak hours, etc.

To find out how sensitive the results are for the number of runs and for the timing of the runs, we carried out an experiment on the data. The results showed that the moment that convergence is obtained for UFP differs from 1 to 18 or 16 runs for Antwerp and Mol, respectively. In fact, a substantial reduction of 70% of the number of runs would still be enough to obtain a reasonable estimate of the overall median concentration, but less so for streets with higher traffic density and a canyon like configuration. A representative estimation of the air quality made on 1 run was exceptional.

The street with the highest traffic density of this study (Plantin en Moretuslei), however, showed the fastest convergence for UFP, probably due to the separate biking lane and the consistently high traffic counts throughout the day. Its convergence pattern was comparable with the pattern found for Kleinendijk in Mol, which is a recreational and green area with very limited local sources. Therefore an a priori definition of a suitable number of runs based on traffic density is hard to

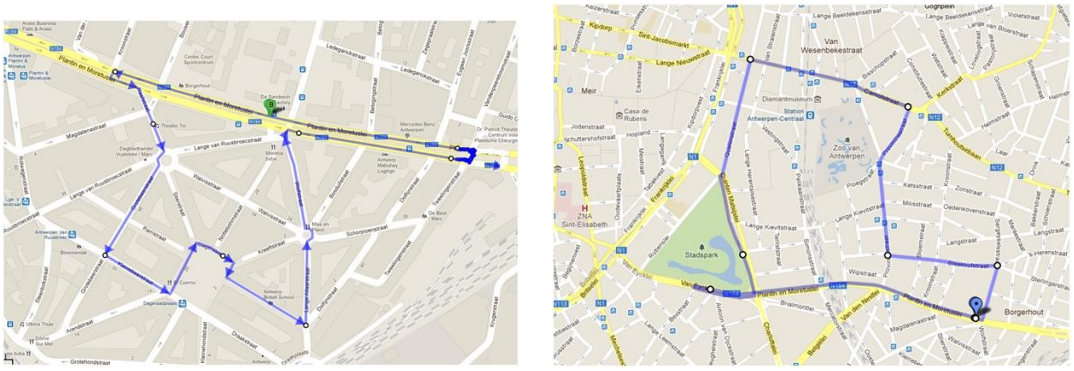

(a) (b)

Figure 2.5: Overview of route 1 and route 2.

make. However, the results indicate that less runs would be needed for streets with low or smooth traffic, whereas more runs are needed in streets with regular periods of congestion. Irrespective of the street and traffic characteristics, the results suggest that it is better to have a spread of the measurement runs over the considered daytime interval and over the entire measurement period, than to have them concentrated. For PM10 the moment that convergence is obtained is generally higher, and the reduction of the number of runs lower (40% in Antwerp, 55% in Mol). This can be explained by the fact that the temporal variability of PM10 at the street is determined by the variability of the local sources but mainly by the variability of the background concentration. In Mol, a median PM10 concentration close to the overall median could be obtained after 10 runs, given that these runs were made on the 10 different dates of the measurement campaign.

Our results indicate that the use of a limited set of about 20 mobile measurements carried out on different days and different times of the day allows to distinguish streets with higher and lower median pollutant concentrations in a significant way. Strictly speaking these relative differences are only valid for the period of sampling, but assuming traffic patterns in all streets are similarly affected by seasonal variations or holiday periods, these differences are indicative for the whole year.

2.2.4 Air quality case study: BC

An exploratory study on the variability, both in space and time, of BC was conducted in Antwerp between 2012-02-13 and 2012-03-08. Measurements were made on a mobile platform –the Aeroflex from VITO (Fig. 2.1)– that was equipped with a BC monitor and additionally equipped with a GPS to register measurement location. The monitoring device and GPS were connected to a netbook to synchronize the sensors and to communicate the data to the central database. BC concentrations (in ng m^{-3}) were measured by the portable micro-aethalometer (Micro Aeth. Model 52, Magee Scientific). The filter ticket was changed at the start of each measurement day, the inlet flow rate was set at 150 ml min^{-1} and a measurement was made each second.

Measurements were made along two fixed routes. The first route was approximately 2 km long, the second 5 km. The starting point of both routes was a central monitoring station from the Flemish Environmental Agency (VMM) at Pantin & Moretuslei. Although both routes passed mainly through residential area, streets and places of different traffic intensity and lay-out were included (Table 2.1).

The first measurement run of the day was always performed around 7 am, just before the morning rush. The last run of the day was performed around 1 pm (Fig. 2.7). A total of 258 runs were conducted along route 1, 112 runs along route 2. Most runs were made on Tuesday and Wednesday, followed by Monday and Thursday (Fig. 2.6). Least runs were made on a Friday. A little less than

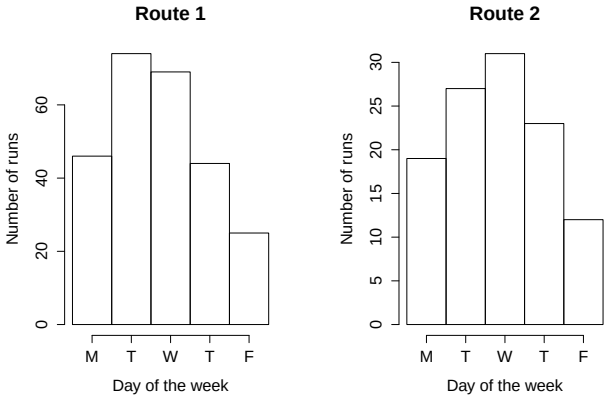

(a) (b)

Figure 2.6: Histogram of the number of measurement runs per day of the week for route 1 (a) and route 2 (b).

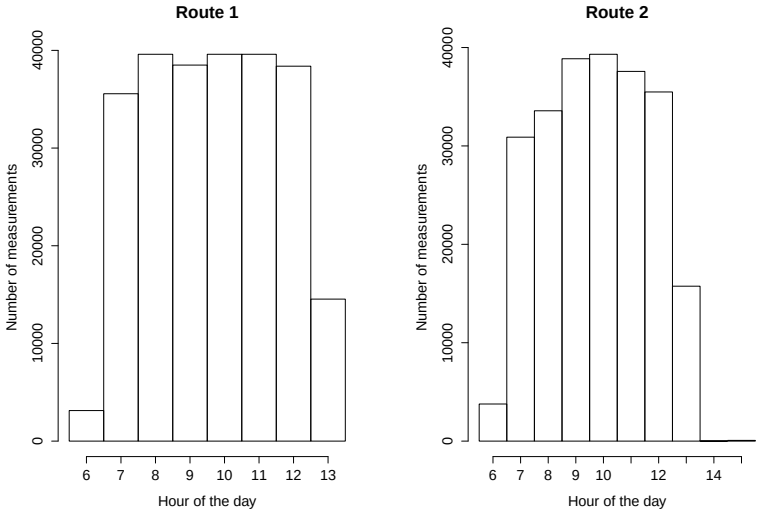

(a) (b)

Figure 2.7: The number of measurement runs per hour of the day for route 1 (a) and route 2 (b).

a quarter of a million measurements were made at both routes over the entire study period.

Please note that the measurements made in this experimental study were not made by the EveryAware SensorBoxes which were unavailable at that time. Yet this case study provides useful information for the EveryAware SensorBox deployment because BC was measured. BC is the primary target air quality parameter for which SensorBox recordings may serve as proxies. Furthermore, during the EveryAware case studies BC will also be measured using the same microaethalometer devices to benchmark the SensorBox measurements. The objective of this section is investigate the dynamics of BC concentrations in an urban environment and to its consequence for data coverage. Both spatial and temporal aspects are highlighted.

Broad scale temporal dynamics To investigate the broad scale dynamics of BC, the data were grouped according to day of the week and according to hour of the day. As such, for each combination a median BC concentration was calculated and plotted (Fig. 2.8). Variations between days and hours of the day were observed. Peak BC concentrations occurred at Monday and Friday morning from 8 until 10 am. The lowest concentrations were observed on Wednesday. Tuesday

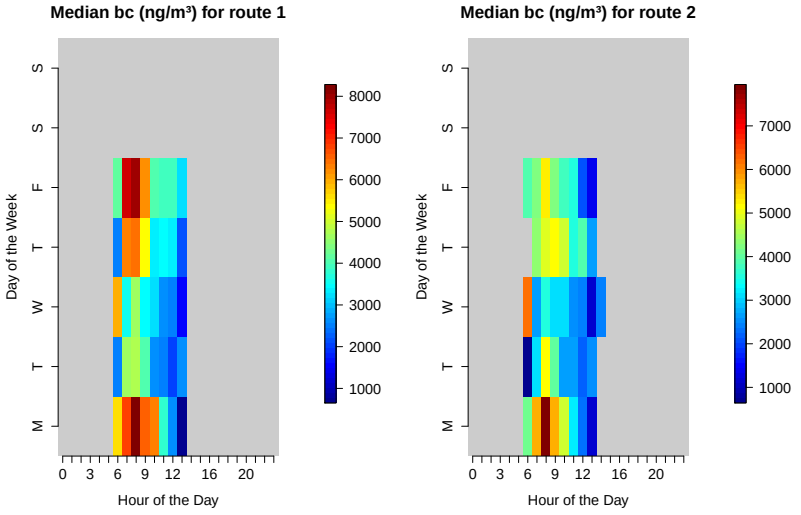

(a) (b)

Figure 2.8: Plot of the median BC concentration in function of hour of the day and day of the week for route 1 (a) and route 2 (b). The gray shaded area represents “no data available”.

and Thursday have median concentrations in between both extremes. The lowest concentrations were as low as 2 μg m^{-3}, the highest >8 μg m^{-3} and >10 μg m^{-3} for route 1 and 2, respectively. From these plot, the high temporal variability is evident and mainly caused by the dynamics of the (traffic) sources.

An important question for the EveryAware project is whether these temporal trends can be obtained from measurement series with lower coverage. Therefore, a small data experiment was set up. From the data sets of both routes, measurements were randomly selected for an increasing data coverage (starting from one measurement per hour of the day and day of the week combination up to 1000 measurements per combination). The trends as observed from the entire data set (Fig. 2.8) are not represented well when only one measurement was used (Fig. 2.9). In this case, the increased concentrations on Monday and Friday are not (well) represented, nor are the differences between hours of the day (rush versus non-rush hours). One observation provides a limited snapshot which, as such, cannot be used to represent the general pattern in BC concentrations. Also 10 observations per day and hour combination still seemed to be a too low number (e.g. elevated Monday morning concentration during rush hours is not visible). From 100 observations on, trends start to appear: a similar variability between hours and days is observed as for the entire data set (Fig. 2.8), although the number of measurements, and therefore the data coverage, is much lower (100 versus several thousands). In conclusion, a coverage of a 100 measurements made at a randomly selected moment in time (within a given hour of the day and day of the week combination) and at a randomly selected location along a fixed route represents broad scale air quality dynamics of a traffic related parameter (BC) satisfactorily.

Spatial variability – streetwise analysis The differences in BC concentration was compared between the streets by a boxplot analysis on all the measurements made in these streets (Fig. 2.10). On route 1 the lowest concentration was observed at Dageraadplaats, the highest concentrations were found in Plantin & Moretuslei and Wolfstraat. A clear connection with traffic may be observed. Dageraadplaats and Korte Altaarstraat are places with low traffic intensities, whereas public transport (busses) pass regularly at Lange Altaarstraat and Wolfstraat. The Plantin & Moretuslei is a 2by 2 lane route with the highest traffic intensities along the biking route. BC concentrations here are generally higher than at places and streets with low traffic intesities. Also the variability between

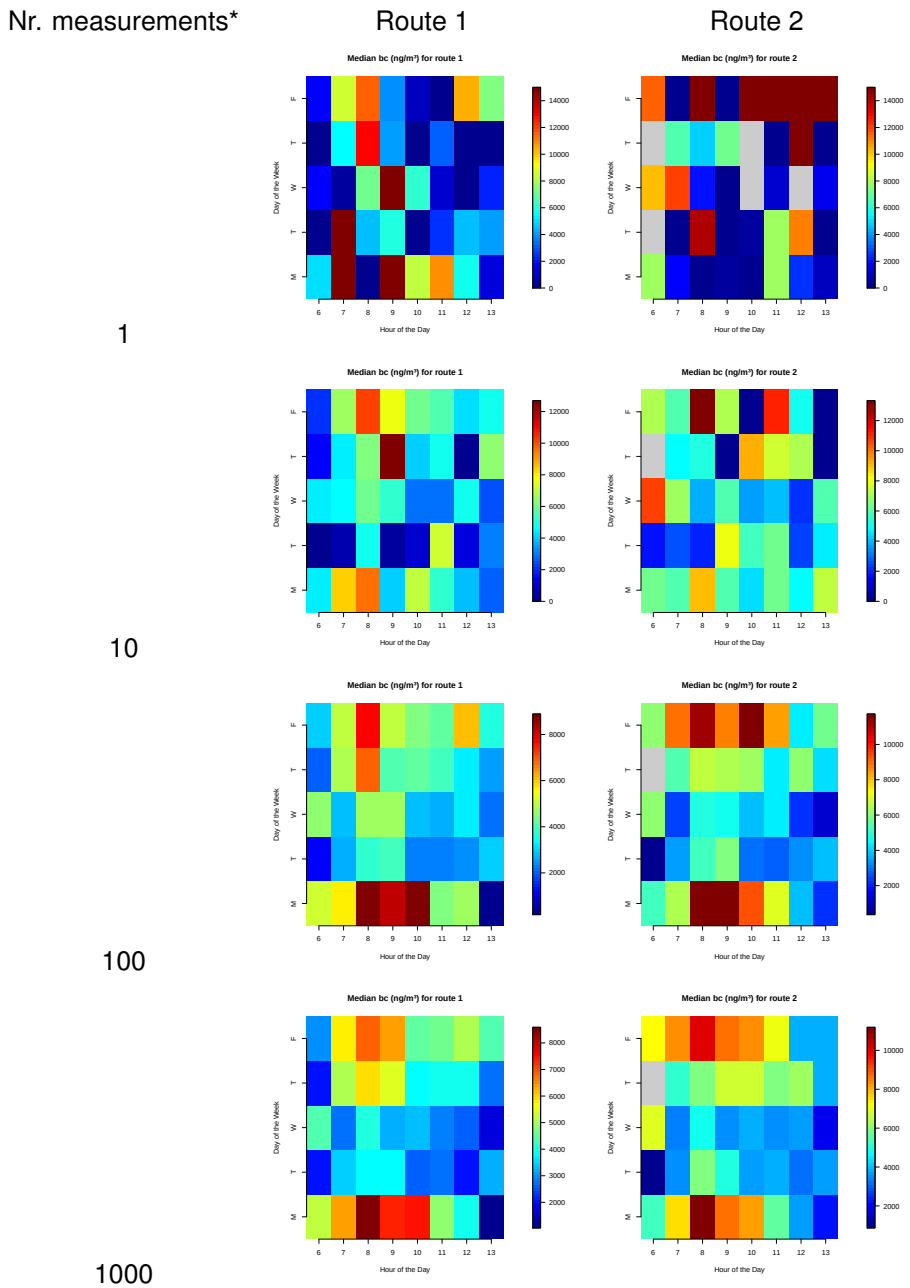

Figure 2.9: Trends between hours and days as observed from a data set with increasing coverage. * The number of measurements randomly taken for each hour of the day and day of the week combiation is given in the left column.

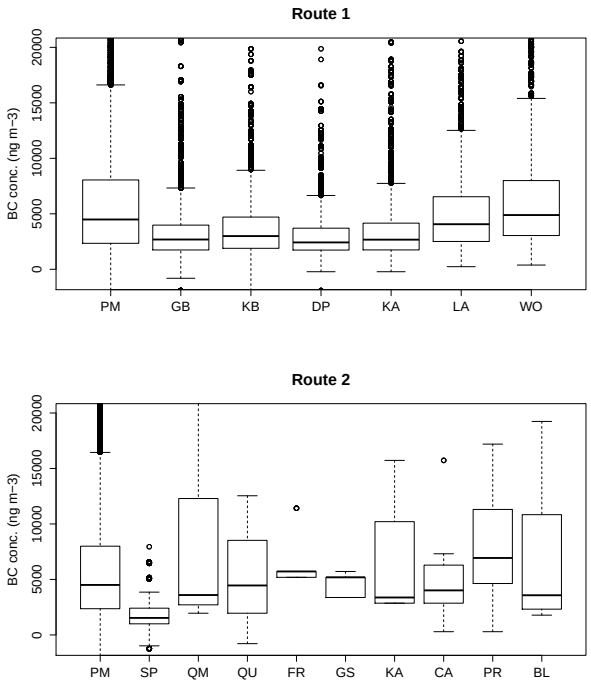

Figure 2.10: Boxplot of BC concentrations in differnt streets on route 1 and route 2. Legend: (route 1) PM, GB, KB, DP, KA, LA, WO are labels for Plantin and Moretuslei, Grotebeerstraat, Kleinebeerstraat, Dageraadplaats, Korte Altaarstraat, Lange Altaarstraat, Wolfstraat, and (route 2) PM, SP, QM, QU, FR, GS, KA, CA, PR, BL are labels for Plantin and Moretuslei, Stadspark, Quinten Matsijsstraat, Quellinstraat, Franklin Rooseveltplaats, Gemeentestraat, Koningin Astridplein, Carnotstraat, Provinciestraat, Bleekhofstraat.

the measurements at a given street, for which the interquartile range of the boxplot is indicative, is much higher at the busy streets (PM, WO, LA) than at the quite streets (DP, KA). This may be caused by (1) temporal fluctuations between hours (low concentrations before and after rush hour, high concentration during rush hours) and (2) temporal fluctuations at a much finer temporal scale (concentration drop right after car passage).

Along route 2, the lowest concentrations were measured at an urban green, Stadspark, where continuous measurements were made during a 5 minute period each run. The highest concentration was measured in Provinciestraat, which is a street canyon with a relative high traffic intensity. At the Franklin Rooseveldplaats, a square with concentrated public transport stops, the BC concentration was also very high with a remarkably low variance between the measurements. Other streets with a high BC concentration are the Quinten Matsijslei, Quellinstraat and Carnotstraat. The BC concentration reached in these streets are higher than or similar to the concentrations measured at Plantin and Moretuslei, the street with the highest traffic intensity along the routes.

Spatio-temporal dynamics A visualisation of the spatio-temporal BC dynamics is given in (Fig. 2.11). These figures stratify the measurements according to the consecutive runs, and indicate the time and location (latitude, longitude). The mapped BC concentrations are shifted in position between the runs to increase the readability of the figures.

There exists a pronounced spatio-temporal variability at both streets. Short peaks in the spatio-temporal series result from a local (both in space and time) increase in BC concentration. These are probably caused by the nearby passage of vehicles in a period of relatively low traffic intensity. The spatial extent of these peaks is a function of the source concentration in the vicinity of the

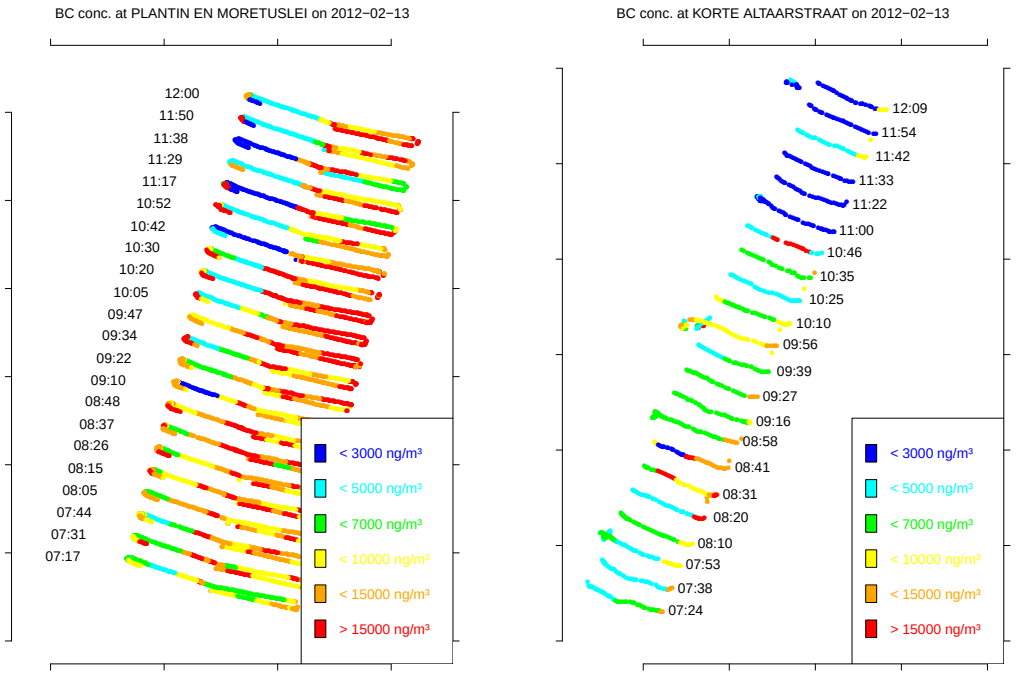

Figure 2.11: BC concentrations at the Plantin & Moretuslei (a) at the Korte Altaarstraat (b) during repeated passage of the mobile monitoring platform on Monday 2012-02-13.

source to the monitoring platform through time (i.e. the movement of the source relative to the movement of the monitoring platform) and the dilution rate.

BC concentration at Plantin & Moretuslei seems to be higher at the eastern side of the street than at the western side. The reason for this difference is unclear at the moment (higher traffic volumes is a possible explanation). Nevertheless, it proves that a measurement at one side would over/underestimate the concentration at the entire street, and therefore stresses the importance of a sufficient spatial coverage.

Such differences within the street were less apparent at Korte Altaarstraat. Apart from a small part of the street at the eastern end, BC concentrations were quite uniform for the entire street for a given period of the day. The increased concentration at the junction with Wolfstraat may be due to the higher concentration of the latter street where traffic intensity is higher and buses pass regularly.

The different goals for data collection in EveryAware are: (1) event-based monitoring, (2) mapping and (3) personal exposure monitoring (see Section 2.1.2). The BC data set under investigation was used to assess the data coverage in relation to the different data collection goals.

→ *Event-based measurements.* Event-based monitoring aims to measure the air quality during a certain event. Event-based monitoring generally requires a targeted data collection. The currently described measurement campaign did not envisage to monitor specific events. One event, however, could be analysed based on these data.

A power generator was placed on a parking space next to the biking lane. The BC measurements clearly reflected this event by highly increased BC concentrations near that location (Fig. 2.12). The systematic way of data collection allowed to identify the start of this event (8 am). The duration of the event, however, could not be assessed because of an incomplete data coverage in time. The generator was still operational when the last air quality measurements at that location were made.

→ *Mapping of urban air quality.* One of the goals of EveryAware is to use air quality measurements

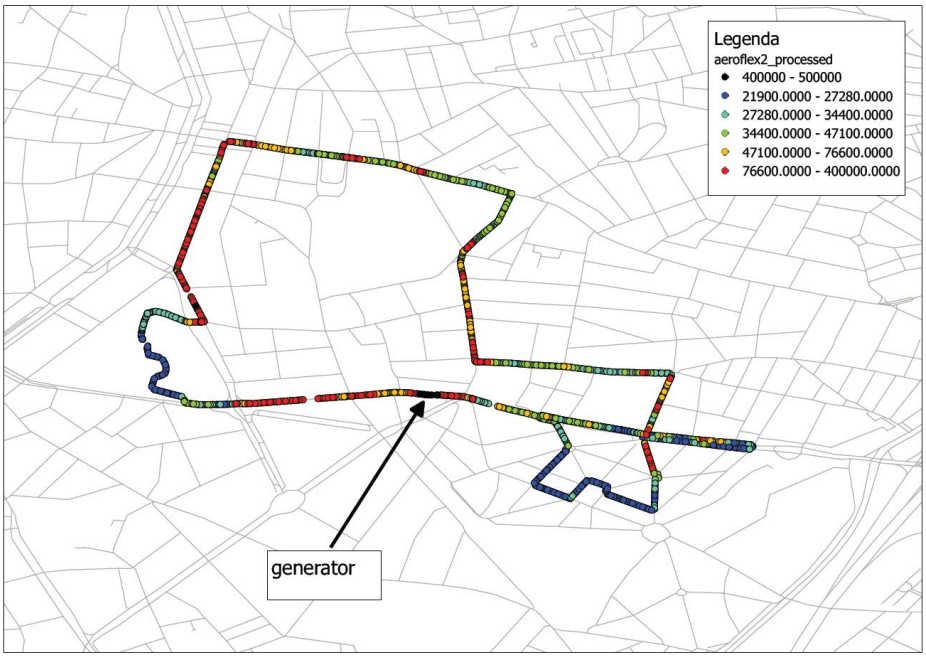

Figure 2.12: Vizualisation of an event: peak in UFP concentration (up to the sensor detection limit of 500000 particles per cc).

to map the air quality of an (urban) area. A school is located on the measurement route at Plantin & Moretuslei. The mobile data were used to quantify air quality during the morning rush (8 – 9 am) in the vicinity of the school entrance. The data coverage requirements for this type of monitoring are straightforward: the spatial coverage is very localized at the school location (fixed point location, or a few points near the school), the temporal coverage should encompass the period between 8 and 9 am. However, the question remains whether the spatio-temporal data coverage on one day is representative for "an average" school day. An average BC concentration of 6000 ng/m^3 was measured during the campaign. Nevertheless, BC concentrations were much higher on several days (e.g. Monday 13/02) and significantly lower on other days (e.g. Wednesday 15/02). This example clearly illustrates the need for repeated measurement to generalize recurring events in time.

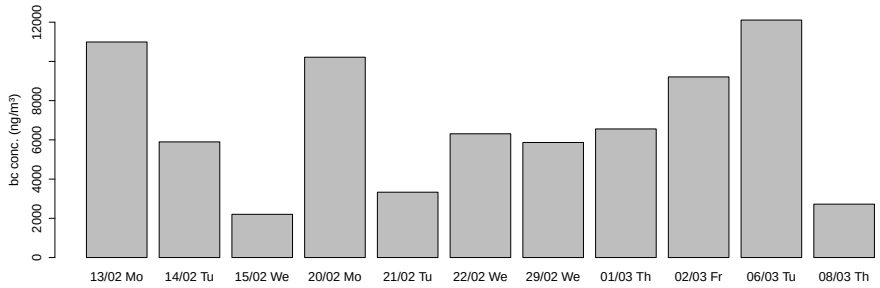

Figure 2.13: Barplot of the BC concentration measured at a school between 8 and 9 am.

→ *Personal exposure monitoring.* Exposure monitoring involves the measurement of air pollution concentrations where a person is exposed to during an activity. The primary purpose of exposure studies is to link air pollution to health effects. In the EveryAware project, however, the focus is on tracking the exposure to pollution, yet without the connection with personal health. The exposure to air pollution is analysed based on high resolution measurements that are made during the

activity/period of interest. Two methods are feasible within EveryAware to reach this goal: (1) a volunteer is equipped with the SensorBox and measures her/his exposure directly, or (2) exposure profiles are computed from high resolution air quality maps which are representative for the route and time of exposure (indirect exposure monitoring). An example of the direct exposure monitoring is given in Fig. 2.14. For direct exposure monitoring the data covers the entire activity pattern, both in space and time. Different transportation modi may be included (pedestrian, bicycle, car, etc.) as well. The indirect exposure monitoring does not allow to include different transport modi.

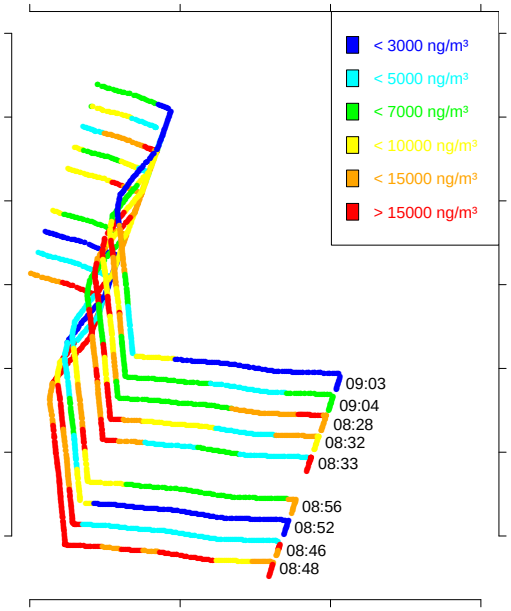

Figure 2.14: Personal exposure to BC along a commuting route (commuting by bicycle).

2.2.5 Pilot case study in Antwerp

During the EveryAware partner meeting in Antwerp (July 9–10, 2012), a test case was set up for air quality and noise measurements in the city center of Antwerp. The test case was deployed on Tuesday July 10th and ran from 10 am until 12:30 pm. A total of 22 people participated in this pilot case, divided over three groups. Each group had one SensorBox at their disposal, and one micro-aethalometer for black carbon concentration measurements for air quality measurements. Air quality measurements were continuously made at a one second time resolution from the start until the end of the test case. Noise measurements were made using smartphones with the Wide-Noise application. Each group had at least 5 smartphones at their disposal. In table 2.2 the test case in Antwerp is summarised.

Each of the three groups received a streetmap with highlighted streets where their focus of measurements should lay. Measurements were made while walking along these predefined routes in a targeted mobile data collection scheme. An overview of the monitoring routes covered by the three teams is given in Fig. 2.15(a), from which the spatial coverage was visually assessed as quite dense within a 1.2 km by 1.2 km wide area in the city center. Fig. 2.15(b) and (c) show the paths recorded by the GPSs connected with the micro-aethalometers and the one recorded with the EveryAware SensorBoxes respectively. The summary of the data coverage is given in Table 2.2.

Table 2.2: Summary of Antwerp cases study.

	Group 1	Group 2	Group 3
Parameters	noise, AQ*	noise, AQ	noise, AQ
Number of meas.	7170	7460	7162
Number of participants	7	7	8
Measurement period			
from	2012-07-10 10:00	2012-07-10 10:00	2012-07-10 10:00
until	2012-07-10 12:30	2012-07-10 12:30	2012-07-10 12:30
Spatial extent			
area	1 by 1 km	1 by 1 km	1 by 1 km
path length (approx.)	3.5 km	4.6 km	3.5 km
Number of streets	9	12	9
Most important streets	Koningin Astridplein, Pelikaanstr., Lange Kievitstr., Q. Matsijsstr., Quellinstr., Frankrijklei, Van Ertbornstr., F. Rooseveltpl., De Keyzerlei	Koningin Astridplein, Pelikaanstr., Simonsstr., P&Mlei, Van Eycklei, Stadspark, Rubenslei, Louiza-Marialei, Frankrijklei, Maria-Theresialei, Quellinstr., De Keyzerlei	Koningin Astridplein, Gemaantestraat, F. Rooseveltplaats, Van Ertbornstraat, Frankrijklei, Maria-Theresialei, Quentin Matsijslei, Lange Kievitstraat, Pelikaanstraat

* air quality

Although the entire case study was spread over two hours time temporal coverage of each location is quite low as the volunteers only passed by once or twice. Even when aggregating to street level most data only relate to one or two passages of a few minutes.

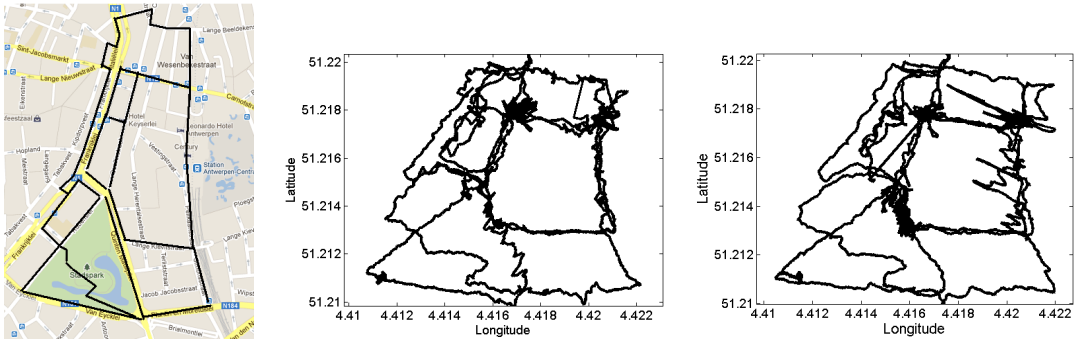

(a) (b) (c)

Figure 2.15: (a) Area covered by the three groups during the Antwerp case study. (b) Path recorded by the GPSs connected with the black carbon monitor. (c) Path recorded by the GPSs present in the EveryAware SensorBoxes.

The maps in Fig. 2.16 are generated using the Kernel $DM + V$ algorithm [Lilienthal et al., 2009], which is a statistical approach to model pollutant distributions. The model is presented in term of four grid maps. The first is a heat map (in [Lilienthal et al., 2009] called a weight map) which depends on the number of measurements per grid location weighted with a Gaussian kernel function. From the heat map a confidence measure for the estimate is calculated at each location. A high value means that the estimate is based on a large number of readings recorded close to the location. A low value, on the other hand, means that few readings nearby the location are available. A third map displays the mean concentration estimate of the target pollutant for grid cells where the confidence is high. A fourth map represents the predictive variance per grid cell, estimating thus the variability of gas readings at each location. The top row refers to the data recorded with the micro-aethalometers. The bottom row refers to the data collected using the EveryAware SensorBox. The blue color refers to low quantities, red color to high quantities and white represents grid cells not covered by the measurements.

From Panels Fig. 2.16(a)-(e), spots with higher data coverage are observed. The top right spot is the starting and ending point for all the groups, where a high number of readings are collected. The other spots refer to locations were one of the groups stopped (for example at traffic light). The difference in structure between the two panels is worth noticing. This is due to different noise in the GPS data. The heat map does not take into account temporal differences. It is not clear if the underlying data all relate to one passage at one specific moment or two passages with e.g.

one hour difference in between them. Panels (b) and (f) show the confidence maps where high confidence (red colour) is given to grid cells for which a large number of readings were recorded in their proximity.

Panels (c) and (g) show the mean concentration maps. Some areas are clearly highlighted. The area on the top centre is a major bus station (Franklin Rooseveltplaats) and confirms the elevated concentrations found in another case study (see Fig. 2.10). Other highlighted spots are more difficult to explain. In general the top left area seems to have higher pollution levels than the right and bottom area. This can be related to the major traffic axes in the former area. Differences between the BC and gas concentration maps are observed. This is mainly due to the fact that the gas sensors in the SensorBox have not been calibrated against the micro-aethalometers yet. Panels (d) and (e) finally show the variance map. The highest variability is observed at locations where the mean concentrations were the highest. The high dynamics of traffic related pollutants at these locations result in the higher variance here.

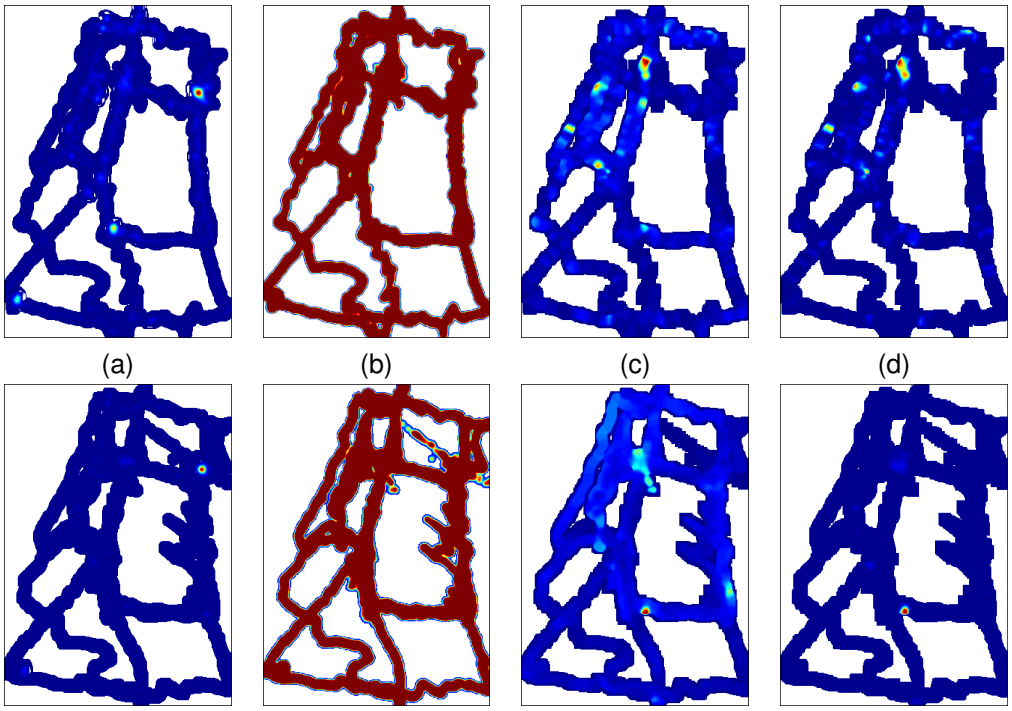

Figure 2.16: Maps computed using the Kernel $DM + V$ algorithm [Lilienthal et al., 2009]. Top row refers to the data recorded with the black carbon monitor. Bottom row refers to the data recorded with the EveryAware SensorBox.(a) and (e) heat maps. (b) and (f) confidence maps. (c) and (g) Mean concentration maps. (d) and (e) variance maps.

This experiment shows that three (groups of) volunteers managed to cover the major roads in a spatially confined area in Antwerp in two hours time. Temporal coverage of the data set is however very limited; in most streets only the teams only passed by once or twice. The resulting map might give some indications on locations with higher and lower air pollution, but this picture is prone to a lot of error and co-incidence. As illustrated in the cases studies above, to draw broader conclusions on air quality in this area such an experiment would have to be repeated on several times in the day and on several days of the week.

2.2.6 Conclusions for set-up of case studies: air quality

Proper data coverage is crucial to make sense of the collected data. Data coverage should be in line with the goals of the measurements and with the spatio-temporal variability of the underlying physical reality. Needed efforts depend further on the type of data collection scheme, and should be in line with the available efforts of volunteers. To have meaningful results the EveryAware case studies should take this into account. The case studies for air quality in EveryAware will show a high similarity with the monitoring campaigns described above. Therefore, several conclusion can be drawn from these experiments to assist the air quality sensor deployment in the case studies with respect to data coverage and data collection schemes.

1. Urban air quality is highly variable in space and time. **Repeated measurements** are crucial to get a representative figure of the air quality. **Mobile collection of data** is the most suitable data collection method to obtain repeated measurements, covering a much larger area than would be obtained by stationary measurements with the same number of SensorBoxes. Single mobile measurement tracks merely give a snap shot. Repeated mobile measurements reveal the high spatio-temporal variability of traffic-related pollution in urban areas and allow to derive representative patterns from the data.

2. It is possible to draw pollution maps or characterise events using mobile measurements, while taking into account spatio-temporal variation. To draw broad scale pollution maps street level **aggregation** is a first useful and in many cases sufficient step. This levels out part of the variability that is related to traffic discontinuity and short-term incidents, but might underestimate intra-street variability. In such case more detailed analysis of the data might reveal the need to divide streets in homogeneous street sections. The impact on air quality of a very local event, both in space and in time, may be characterized by a limited set of measurements. Spatial and temporal aggregation might in that cases allow for much more detail. Recurrent events can only be characterised by repeated measurements as the impact of the event might strongly depend on e.g. meteorological conditions.

3. A **data collection scheme** with a person taking the same route on different moments of the day repeated 20 times on different moments of the days in a three weeks period will be sufficient to reveal the major daytime hot spots on this route, and relative differences between different street sections on the route, i.e. when the underlying diurnal traffic patterns are similar for the streets. Increasing data by increasing the number of runs will allow to aggregate the data at a more detailed level, i.e. distinguishing non-homogeneous street sections and intersections, and aggregating data in relevant time intervals, e.g. hourly averages, peak and off-peak hours. Street characteristics such as traffic dynamics and street architecture and configuration, have a large effect on the data coverage requirements. Streets with low or smooth traffic require much less measurements than busy routes with varying periods of congestion.

4. Statistical power will increase when all runs are carried out at more or less the same time, e.g. a commuter taking the same road to work every day. On the other hand the data might not be representative for other periods of the day. In the case of the commuter it will only possible to draw conclusions on the road taken.

5. Whereas the data can be put in a comparative perspective (e.g. comparing different locations), it is far more challenging to conclude on actual average concentration levels during the measurement period, and, because of clear seasonal effects, even more to extrapolate these average levels to other periods. To do so measurements would have to be repeated in different seasons.

6. Three volunteers can cover the major roads in a spatially confined area of 1 to 2 km^2 in a busy city centre in two hours time. Whereas this might already give indications of hot spot areas or broad patterns of air pollution, the results from such an exercise are prone to a lot of error and co-incidence. This experiment would have to be repeated according to the guidelines set out above to be able to draw conclusions.

7. Taking into account the large data needs to get a representative picture of urban air quality and the fact that, both because of its cost and its technical complexity, the SensorBoxes will be distributed to a rather limited group of people (as opposed to the Widenoise app), data collection should **focus** on a clearly defined time frame and area in order to obtain sufficiently repeated air quality measurements (e.g. air quality in the streets around a school , exposure of cyclists to air pollution on a major access route to the city during traffic peak hours). This calls for a **targeted data collection approach**. Broad scale city-wide mapping exercises require opportunistic approaches with a measurement device that measures continuously with minimal intervention of the user. This is not the case at this moment for the EveryAware SensorBox.

2.3 Noise monitoring

2.3.1 Introduction

Noise is a term that people use to refer to sounds that are somehow *unwanted*. The labelling of particular sounds as noise, and thereby as unwanted, may be influenced as much, and sometimes more, by personal opinion and contextual and cultural factors[1], than by physically measurable properties of the sound in question [Stevens, 2012, Chapter 4]. Despite being a subjective topic there is ample scientific evidence that noise is an increasingly pressing problem around the world, especially in urban areas. Long-term, excessive exposure is known to have negative effects on human health, well-being and productivity [European Commission, 2011; WHO Regional Office for Europe / European Commission Joint Research Centre, 2011]. Hence the notion that noise is an environmental pollutant and a health hazard, rather than just a nuisance, has become widely accepted in recent decades [Goines and Hagler, 2007].

Generally speaking, noise can be problematic where and whenever the produced sound level, the number of sources, the spatio-temporal scale of exposure, the number of exposed individuals and/or the objectively or subjectively observed harm is deemed too high. Typically a distinction is drawn between two categories of noise (problems): *occupational noise* and *environmental noise*. Occupational noise is the noise people are confronted with in the context of their job. Within the context of the EveryAware project we focus exclusively on the problem of environmental noise. Environmental noise is the noise people are exposed to in their daily lives as a result of various human activities, such as those related to transport, industry and leisure[2]. Figure 2.17 shows a powerful example of environmental noise, in this case caused by transport activity.

Figure 2.17: Environmental noise illustration: a Boeing 747-400 flying low over residential housing while approaching London Heathrow Airport, England, UK.

[1] After all *one person's music is another person's noise*.

[2] Note that often the same activity can be seen as both a source of occupational noise (i.e. for those who are exposed in their professional capacity) and environmental noise (i.e. for all other exposed people).

2.3.2 Spatial and temporal variability of urban noise

The acoustic properties of urban soundscapes[3] are highly dynamic in both space and time.

Similarly to air quality, environmental noise is influenced by urban topography and topology (e.g. buildings and other objects can reflect sound waves), surface types and vegetation, as well as by atmospheric conditions (e.g. wind speed and direction).

What differentiates noise from air pollutants is the temporal and spatial reach. Whereas air pollutants can stay in the atmosphere for very long periods after being emitted, noise dies out almost instantaneously after the source stops producing it. Whereas some types of air pollutants can cause degraded air quality hundreds of kilometres away from their source, the effects of environmental noise are typically limited to a few kilometres around the source. Another noteworthy difference is the importance of human factors. Whereas many (potentially) harmful air pollutants cannot be smelled or seen, noises need to be audible in order to be harmful, and whether they are (or are perceived as such) is influenced by many factors, including non-acoustic ones.

Before we discuss how urban noise can be monitored or otherwise assessed we should clarify what exactly is being measured and what that means. We also touch upon the regulatory framework.

What to measure

When assessing environmental noise the primary (and usually the only) acoustic parameter that is taken into consideration is *sound* (*pressure*) *level*, which is expressed in decibels (dB).

It is important to differentiate between sound level and *loudness*: the former is a physical property of sound that can be directly measured, whereas the latter is a psychological term referring to the attribute of auditory sensation in terms of which sounds can be ordered on a scale extending from "quiet" to "loud". Although sound level is the main factor that influences loudness it is not the only one. Another factor is sound frequency, because human hearing is not equally sensitive at all frequencies[4]. For this reason sound level measurements are typically adjusted based on the frequency distribution of the sound in a process is called *frequency weighting*. For the assessment of environmental noise the de facto weighting to use is *A-weighting* [International Electrotechnical Commission, 2002; International Organization for Standardization, 2003, 2007], in which case measurements are expressed in dB(A). However psychoacoustic research has shown that, besides sound level and frequency, loudness perception is also influenced by other acoustic and non-acoustic (subjective/contextual) factors. Moreover, the relation between loudness and annoyance, and any physical or mental harm, is very complex as well [Florentine et al., 2011].

The message here is that although measuring – or predicting (see below) – (A-weighted) sound level is the de facto approach to assess environmental noise, this type of data is limited at best when it comes to capturing or explaining the subtleties of sound perception (loudness, annoyance, etc.) and to estimate physical and mental harm caused.

Regulatory framework & official assessment efforts

Recommendations or regulations aimed at limiting noise exposure are typically specified as A-weighted sound level averaged over multiple hours. For instance, the World Health Organisation (WHO) recommends that the average A-weighted sound level (denoted as L_{Aeq}) over the 16 hour day and evening period should not exceed 55 dB(A) outdoors, and 50 dB(A) inside dwellings. To avoid sleep disturbance the WHO advises that nightly averages should stay below 40 dB(A) outside, and below 30 dB(A) inside bedrooms [WHO, 1999; WHO Regional Office for Europe, 2009].

[3] The term *soundscape* was coined by [Schafer, 1969] as the auditory equivalent of a landscape – i.e. the whole of sounds and noises that is characteristic for a certain place and/or time.

[4] I.e. sounds with the same level but different frequencies can be perceived to have different loudness.

Due to recommendations such as those made by the WHO, the regulatory framework concerned with the assessment of environmental noise usually takes a long-term perspective. For example, Directive 2002/49/EC, better known as the *Environmental Noise Directive* (END), obliges EU member states to produce so-called *strategic noise maps* for major cities [European Parliament and Council, 2002]. Separate maps must be produced for different sources of noise, namely road, rail and air traffic and industry. For every source 2 maps must be produced one representing L_{den} (a weighted average of L_{Aeq} taken over 24 hours, with a bias for evening and night time noise) and the other L_{night} (L_{Aeq} taken over 8 night hours). These maps are valid for 5 years and represent the average sound level one can expect for a limited number of environmental noise sources on an average day in the year of study. Hence, they do not cover individual, incidental, local or short-term events (e.g. roadworks, sirens, noisy neighbours, etc.).

In the European Union, large-scale assessments of urban noise conducted by officials typically involve few field measurements and instead rely on simulation models[5]. The main reason is scalability: it is infeasible to measure the sound level at all places and times. To predict levels at different places and times they use specialised software which employs source-specific sound propagation models that are fed with statistics about the presence of considered sources (e.g. average number of vehicles on roads, frequency of planes on low-altitude flight paths, etc.) and information on urban topology (e.g. height of buildings, surface type of roads, presence of noise barriers, etc.).

Alongside the production of simulation-based noise maps some local authorities also operate a network of sensors which allow them to measure (rather than predict) the sound level at a limited number of places over extended periods of time. Examples of such networks can be found in the cities of Brussels and Paris, as wells as around some major airports. However, due the high cost of the equipment used, this approach has limited scalability.

Finally environmental agencies (or their subcontractors) sometimes conduct small-scale, short-term acoustic studies at specific places. Such efforts may be aimed at assessing a local problem, possibly in response to complaints by citizens. Alternatively the goal may be to collect data to initialise or validate modelling efforts. Fieldwork and analysis are carried out by professionals using specialised (i.e. expensive) equipment and software. As with sensor networks this approach has limited scalability: authorities simply do not have the means to let their personnel carry out measurements everywhere and all the time.

An opportunity for crowd-sourcing

As demonstrated in earlier work, citizen science [Ellul et al., 2011; Francis et al., 2008] and mobile sensing [D'Hondt et al., 2011; Stevens, 2012] present an opportunity to complement the efforts of officials with urban noise data collected by citizens. This approach allows the assessment of urban noise using measurements rather than predictions and is cheaper than setting up dedicated sensor networks or employing professionals to do fieldwork. Although the tools (i.e. cheap sound level meters or mobile phones) cannot offer the same level of accuracy this problem can be offset through calibration and by aggregating and averaging larger sets of measurements over space and time [Stevens, 2012, Chapter 7]. Crowd-sourcing also allows to capture of more than just sound level: through social tagging and perception ratings citizens can build a richer representation of the urban soundscape, perhaps providing a better understanding of the more intangible human factors that, as noted above, play an important component in noise.

As with air quality monitoring, the spatial and temporal coverage that is achievable when monitoring urban noise via crowd-sourcing depends on the goal, the number and commitment of contributors and whether (and how) the work is coordinated. In principle, event-based measurement, local

[5]The END is clearly written with this approach in mind. For instance, the requirement to make separate maps per sound source is difficult to fulfil with measuring since sound level meters cannot differentiate between sources.

area[6] mapping and personal exposure monitoring are all possible, but may fail if the resources (in terms of human effort and organisation) fall short.

[Stevens, 2012] argues that small to medium-scale data collection campaigns, conducted by people that know and trust each other, and involving a targeted data collection scheme or protocol (aimed at answering specific questions and aligned with local concerns) – called *group sensing* initiatives – are more feasible and effective than large-scale campaigns involving hundreds of individuals who are mostly strangers to one-another and who operate without coordination and may have diverse motivations – called *mass sensing* initiatives.

2.3.3 EveryAware pilot cases

This section presents an overview of the data coverage of the EveryAware pilot studies for noise measuring. All of these were carried out using the WideNoise App for Apple iOS or Android devices. It is important to note here that, unlike with the early air quality coverage assessment described earlier in this document, which made use of a diverse range of sensors whilst the EveryAware SensorBox itself was being constructed, it was possible to conduct these studies with the WideNoise App itself. Thus rather than providing a theoretical 'best' answer to the data coverage issue, these studies permit preliminary investigations into what is possible to achieve using crowd-sourced approaches and tools (the WideNoise App) that pre-date the EveryAware project.

Overall Worldwide WideNoise measurements

The currently collected noise measurement data (from the launch of the App until the 23th August 2012) is summarized in Table 2.3. There are nearly 25,000 measurements taken so far. Not every noise measurement was associated with geo-coordinates. As the cell phone does not always have access to a location provider, a significant number of samples have been captured without specific coordinate information as can be seen from the table. Using the ip address at least estimates can be made on the user's location leaving only a small amount of measurements without geo-coordinates. Such measurements could also be associated with a set of tags. Tags can be added by the user after the noise measurement has been taken.

Each measurement spans five seconds. It can be extended to ten or 15 seconds by the user while the measurement is taken. The coverage section of the table shows the time covered by the measurements. They cover nearly 42 hours. For the distribution of durations please refer to Figure 2.18(b).

The table also covers statistics concerning WideNoise ids addressing questions similar to the single measurement statistics: How many users tag? Which smartphone brands are used?

Finally, the table aggregates the measurements and presents certain statistics on the average decibel (dB) values of the measurements. The average decibel values are calculated by the WideNoise cellphone application and need to be handled with care (See D1.1 for details).

Figure 2.18 shows several of the statistics from Table 2.3 as pie charts. Figure 2.18(a) shows the relative amounts of measurements with and without geo-coordinates. Figure 2.18(b) shows the relative amounts of measurement durations. Figure 2.18(c) shows the relative amounts of measurements with attached tags, with attached Twitter timelines, with none of those two attachments and with both. Figure 2.18(d) shows the same as Figure 2.18(c) restricting samples to those with geo-coordinates. Finally, Figures 2.18(e) and 2.18(f) show the relative amount of measurements made by Apple products against the measurements made by Android products once with and once without geo-coordinates. In general, the majority of the measurements were made by Apple products over a 5 seconds interval. The majority of the data had geo-coordinates but no tag or perception annotation.

[6] Typically a few streets or a small neighbourhood, rather than a large city.

Data	
Location	worldwide
From	2011-12-08 17:14:58 CEST
Until	2012-08-23 11:00:32 CEST

Measurements	
Number of measurements	24886
Number of measurements with geo-coordinates	17011
Number of Measurements with geo-coordinates from ip	7627
Number of measurements with tags	3647
Number of measurements with perceptions	8015
Number of WideNoise ids from Apple products	19105
- with geo-coordinates	11578
Number of WideNoise ids from Android products	5781
- with geo-coordinates	5433

Coverage	
Overall duration of measurements	41:31:25

WideNoise Ids	
Number of WideNoise ids	8346
Number of WideNoise ids with geo-coordinates	4353
Number of WideNoise ids with geo-coordinates from ip	4480
Number of WideNoise ids with tags	284
Number of measurements with perceptions	2202
Number of WideNoise ids from Apple products	7972
- with geo-coordinates	4026
Number of WideNoise ids from Android products	375
- with geo-coordinates	328

Decibel Statistics	
Average	63.94
Standard deviation	19.27
Minimum	0
Maximum	119.89

Table 2.3: Worldwide WideNoise Summary.

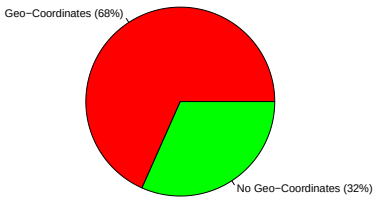

(a) Measurements with and without geo-coordinates for worldwide data.

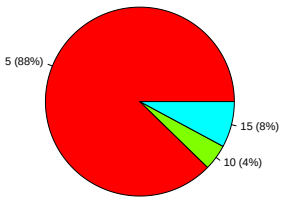

(b) Measurement durations for worldwide data.

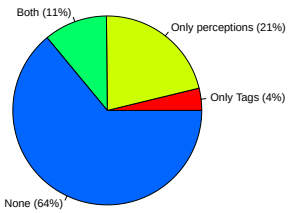

(c) Measurements with either tags, a perceptions, none, or both for worldwide data.

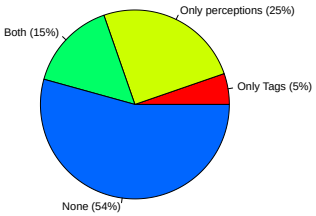

(d) Measurements inlcuding geo-coordinates with either tags, perceptions, none, or both for worldwide data.

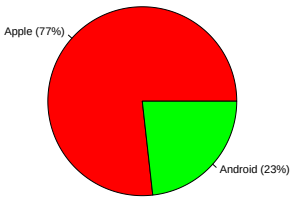

(e) Measurements from Apple and Android products for worldwide data.

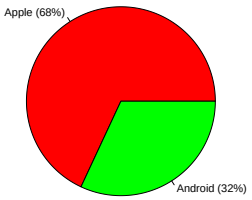

(f) Measurements from Apple and Android products with geo-coordinates for worldwide data.

Figure 2.18: Pie charts summarizing several statistics for worldwide noise measurements.

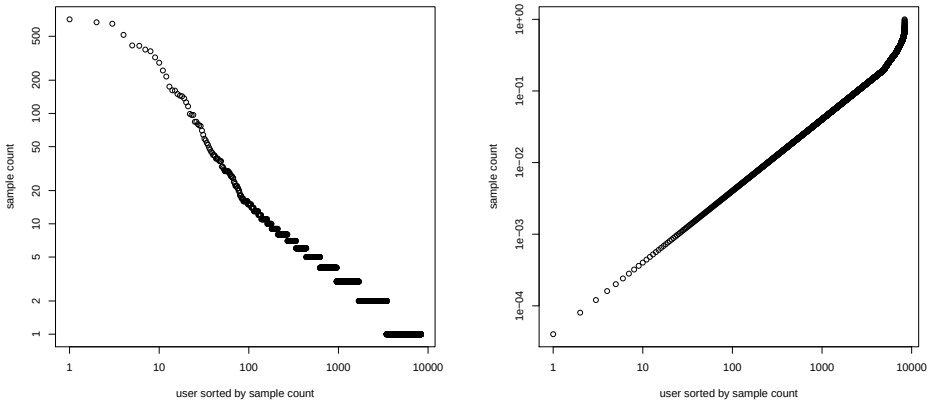

(a) Measurements per user using a log-log plot. (b) Measurements per user smoothed by summing up the frequencies per user.

Figure 2.19: Measurements per user for worldwide data.

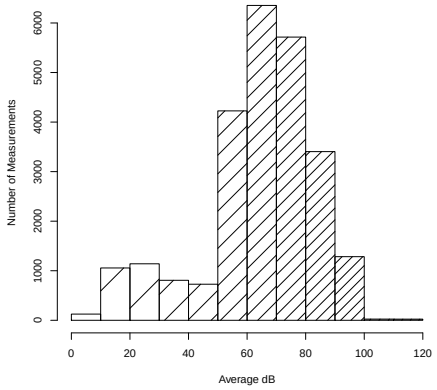

Figure 2.20: Noise Histogram for worldwide data.

To illustrate how user activity is distributed, Figure 2.19 shows two log-log plots of the users sorted by frequency descending on the x-axis. For Figure 2.19(a) the number of measurements for each user is directly plotted to the y-axis. For Figure 2.19(b) the frequencies for the user as well as all preceding users frequencies are summed up. Both figures show that only a small amount of users contribute many measurements while a large amount of users will only take very few samples.

Figure 2.20 provides a histogram with 10 dB sized bins summarizing the overall distribution of decibel values. Note how the main body of measurements provides average dB values between 60 and 70 dB.

A list of top ten tags by count as well as their average geo-coordinates are listed in Table 2.4.

The smartphone application also asks the user to add perceptions to their measurements. Those are summarized in Table 2.5. A perception value always ranges from 0 to 1, with 0.5 as the default value. A perception is specified by two words. If the perception value is closer to 0 the first word is weighted more. If the value is closer to 1, the second word is weighted more. Thus, if the user does not change the perception values a value of 0.5 will be submitted. The table accounts for this by giving an overall average as well as an average excluding the default values.

Finally figures 2.21 and 2.22 show snapshots of the WideNoise map as available on the case study

Tag	Count	Average Longitude	Average Latitude
garden	558	-0.25	51.46
heathrow	342	-0.65	51.38
aeroplane noise	319	-0.67	51.38
Antwerpen	249	4.42	51.21
car	215	4.90	50.07
street	146	6.01	48.44
plane	142	-0.30	51.47
station	138	4.39	51.14
traffic	135	3.36	50.34
office	103	8.32	49.04

Table 2.4: Top ten tags by count for worldwide data.

Perception	Overall Average	Amount (non 0.5)	Average (excluding 0.5)
Love / Hate	0.53	5353	0.66
Calm / Hectic	0.53	5359	0.62
Alone / Social	0.50	5316	0.48
Nature / Man-Made	0.59	7019	0.83

Table 2.5: Perceptions for worldwide data.

homepage[7]. The map summarizes the measurements by depicting clusters as in Figure 2.21 or by sorting measurements into a grid as in Figure 2.22. The colors correspond to decibel value intervals as follows:

- below 40 dB: blue
- above 40 dB: green
- above 60 dB: yellow
- above 70 dB: light orange
- above 80 dB: orange
- above 90 dB: red
- above 100 dB: purple

Beta Test 1 - London Citizen Cyber Science Workshop

The aim of the beta test on noise monitoring was to test recruitment methods as well as to receive informal feedback on the usability of the WideNoise application. The beta test was held at the London Citizen Science Summit in February 2012. The beta test was aiming to recruit the conference delegates by asking them to download the WideNoise application and use it to carry out noise mapping around the conference facilities. The summit lasted for 3 days, on the first day 133 readings were created by the delegates, on the 2nd 157 recordings were made, and on the final day a further 165 readings were created. Out of the total 41 measurements had at least one tag and 157 measurements had associated perception ratings. The average of decibel level for these readings at the beta test was 60.8 dB. More information about the beta test can be found in deliverables 3.1 and 6.3.

[7] http://cs.everyaware.eu/event/widenoise/map

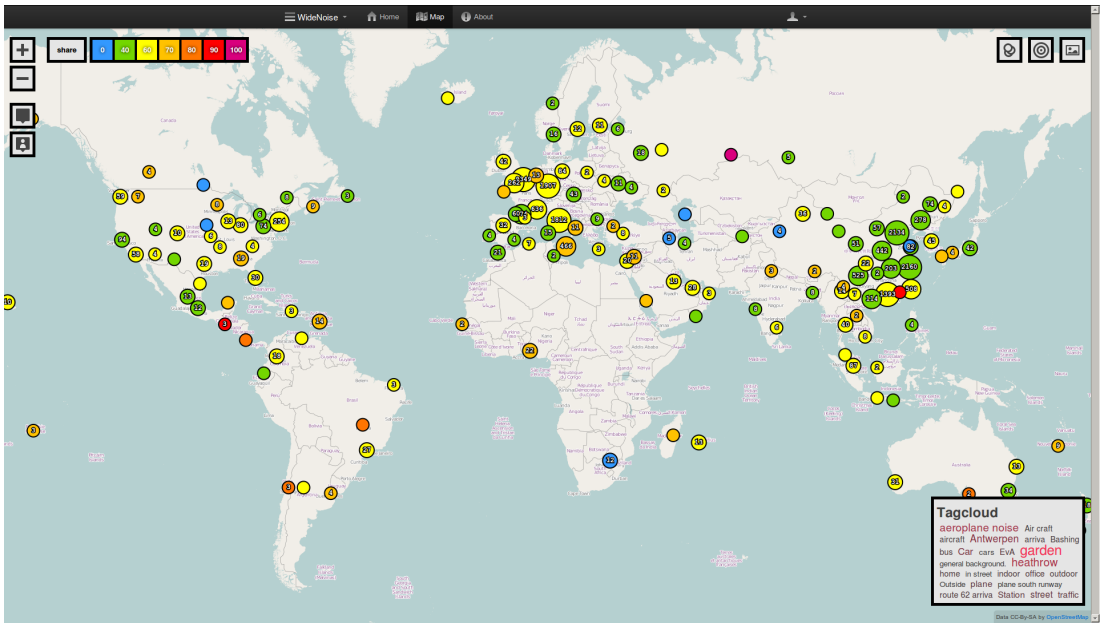

Figure 2.21: WideNoise map showing clusters.

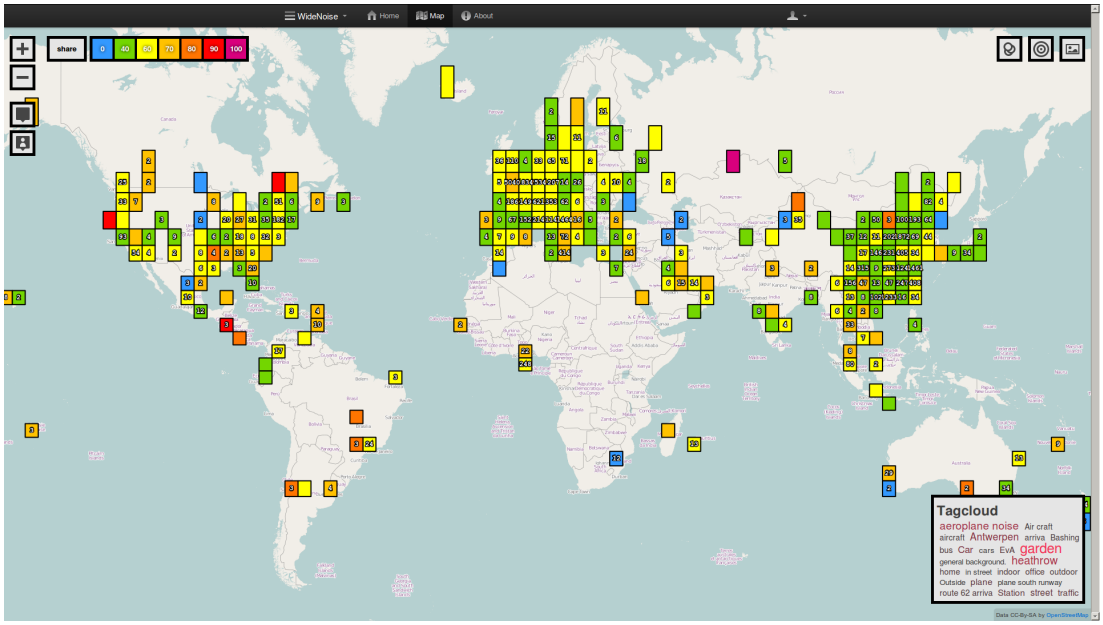

Figure 2.22: WideNoise map showing grid.

Figure 2.23: Heatmap of the noise measurements conducted in the pilot case in Rome.

Additional Coverage Tests - Rome

The noise measurement data from a case study in Rome is summarized in Table 2.6. The case study focuses on the 9th of June, 2012 and on a square area in Rome roughly covering 0.66 km^2. There were close to 700 measurements taken in merely eleven hours. Because we focus on a particular area, there are no samples without geo-coordinates. None of the geo-coordinates was inferred by ip. There where not many tagging and perception annotations. A heat map showing the density of the measurements is shown in Fig. 2.23.

Each measurement spans five to fifteen seconds as mentioned in Section 2.3.3. The measurements were able to cover a time of one hour, three minutes and five seconds. Most users did not take advantage of extending the sample though (see Fig. 2.24(a)). Assuming a radius of 10m the measurements cover around 0.11 km^2 which amount to about 13.75 % of the area.

The table also covers statistics concerning WideNoise ids. There was a relatively small number of users. Nearly all of them added perceptions but only half of them used the tagging feature. The smartphone OS brand usage was equally distributed.

Finally, the table aggregates the measurements and presents certain statistics on the average decibel (dB) values of the measurements (see Section 2.3.3). Comparing with Table 2.3 the average is a little higher and the standard deviation lower. This can be explained by the fact that measurements are taken in a city (as compared to everywhere) and concentrated on a relatively small area.

Fig. 2.24 shows several of the statistics from Table 2.6 as pie charts. Fig. 2.24(a) shows the relative amounts of measurement durations. Fig. 2.24(b) shows the relative amounts of measurements with attached tags, with perceptions, with none of those two attachments and with both. Finally, Fig. 2.24(c) shows the relative amount of measurements made by Apple products against the measurements made by Android products. Note how the distribution greatly differs from the overall distribution from 2.18(e).

To illustrate how user activity is distributed, Fig. 2.25 shows two log-log plots of the users sorted by frequency descending on the x-axis. For Fig. 2.25(a) the number of measurements for each user is directly plotted to the y-axis. For Fig. 2.25(b) the frequencies for the user as well as all preceding users frequencies are summed up. Fig. 2.26 provides a histogram with 10 dB sized bins summarizing the overall distribution of decibel values. Compared to Fig. 2.20 the bins in the lower dB intervals are smaller relative to the bins in the 60 dB area. Just like the higher average dB value this indicates that cities are louder than when considering the overall dB distribution.

A list of top ten tags by count are shown in Table 2.7. As in Table 2.5 the perceptions for Rome are listed in Table 2.8.

Finally figure 2.27 shows snapshots of the WideNoise map as available on the case study home-

Data	
Location	Rome
From	2012-06-09 09:34:25 CEST
Until	2012-06-09 20:57:37 CEST
Minimum Longitude	12.5108470
Minimum Latitude	41.8912730
Maximum Longitude	12.5190240
Maximum Latitude	41.9023060
Area	0.8 km^2
Measurements	
Number of Measurements	676
Number of Measurements with geo-coordinates from ip	0
Number of Measurements with tags	77
Number of Measurements with perceptions	180
Number of Measurements from Android products	444
Number of Measurements from Apple products	232
Area	0.66 km^2
Coverage	
Overall duration of measurements	1:3:5
Area coverage (radius 10m)	0.09 km^2
Area coverage (radius 10m)	14.12 %
WideNoise Ids	
Number of WideNoise ids	15.00
Number of WideNoise ids with geo-coordinates from ip	0.00
Number of WideNoise ids with tags	8.00
Number of WideNoise ids with perceptions	13.00
Number of WideNoise ids from Android products	8.00
Number of WideNoise ids from Apple products	7.00
Decibel Statistics	
Average	68.82
StD	7.15
Minimum	42.29
Maximum	92.08

Table 2.6: Rome WideNoise Summary.

Tag	Count
outdoor	34
street	27
car	21
voice	13
indoor	12
wind	6
birds	5
bookstore	5
music	4
quiet	4

Table 2.7: Top ten tags by count for the Rome data.

Perception	Overall Average	Amount (non 0.5)	Average (excluding 0.5)
Love / Hate	0.53	129	0.53
Calm / Hectic	0.53	71	0.48
Alone / Social	0.50	104	0.67
Nature / Man-Made	0.59	166	0.69

Table 2.8: Perceptions for the Rome data.

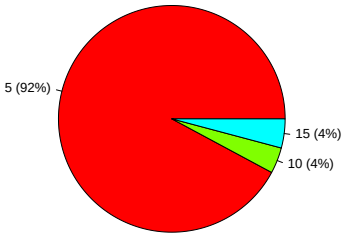

(a) Measurement durations for the Rome data.

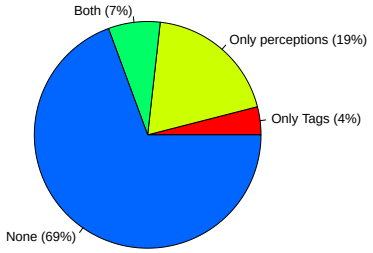

(b) Measurements with either tags, a perceptions, none, or both for the Rome data.

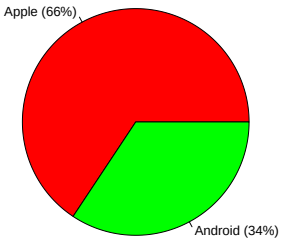

(c) Measurements from Apple and Android products for the Rome data.

Figure 2.24: Pie charts summarizing several statistics for worldwide noise measurements.

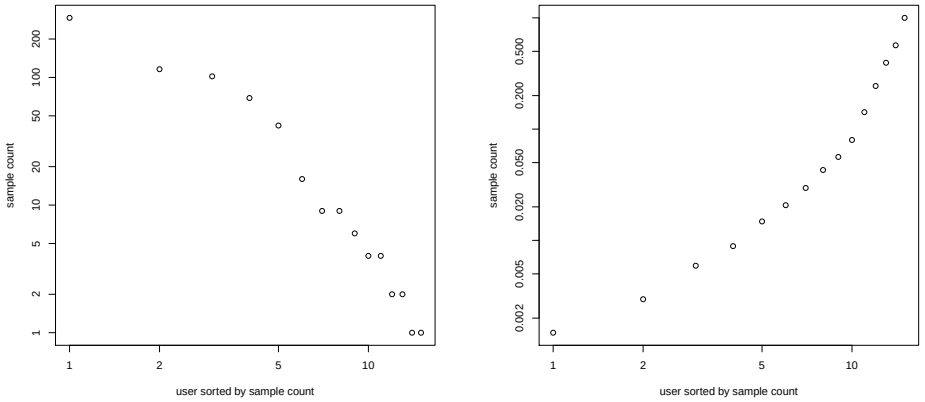

(a) Measurements per user using a log-log plot. (b) Measurements per user smoothed by summing up the frequencies per user.

Figure 2.25: Measurements per user for the Rome data.

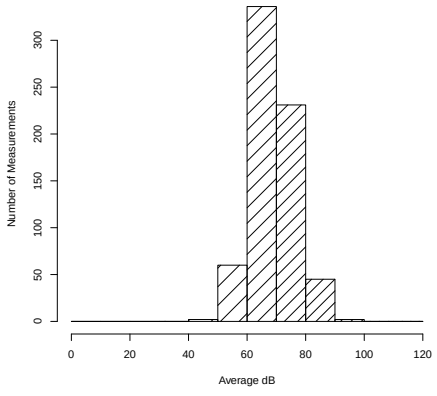

Figure 2.26: Noise Histogram for the Rome data.

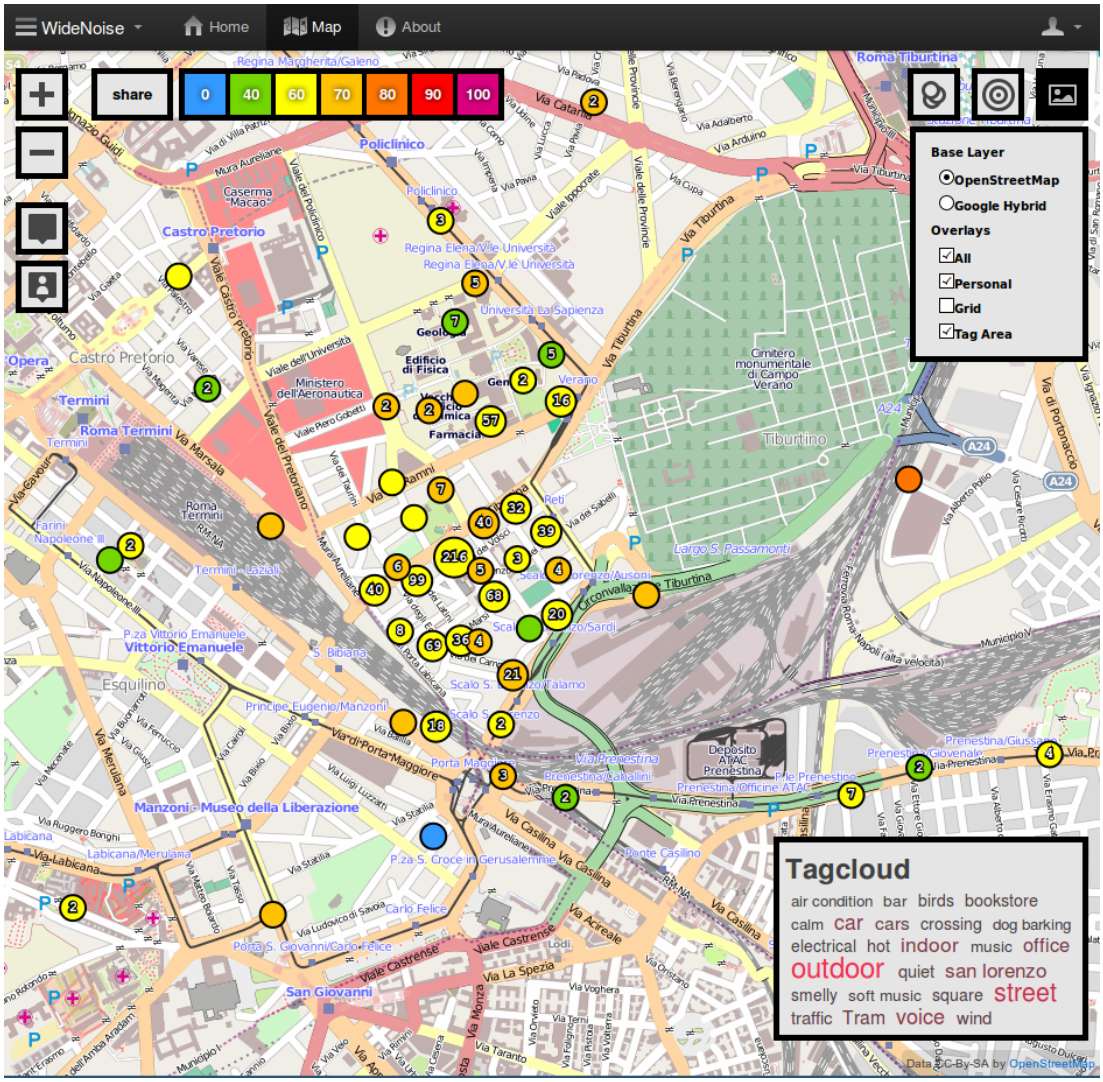

Figure 2.27: WideNoise map showing clusters for the Rome data.

page [8]. The map summarizes the measurements by depicting clusters. For details on the colors coding see Section 2.3.3.

Additional Coverage Tests - Antwerp (July 10th, 2012)

The noise measurement data from a case study in Antwerp is summarized in Table 2.9. The summary is similar to the one in Section 2.3.3.

The case study focuses on the 10th of July, 2012 between 9:30 and 13:00 o'clock and covers a square area in Antwerp roughly covering 2.6 km^2. There were close to 1200 measurements taken in merely three and a half hours. Because we focus on a particular area, there are no samples without geo-coordinates. None of the geo-coordinates was inferred by ip. There where not many tagging and perception annotations.

Each measurement spans five to fifteen seconds as mentioned in Section 2.3.3. The measurements were able to cover a time of one hour, 38 minutes and 55 seconds. Most users did not take advantage of extending the sample though (see Figure 2.28(a)). Assuming a radius of 10 m the measurements cover around 0.2 km^2 which amount to about 7.45 % of the area.

[8] http://cs.everyaware.eu/event/widenoise/map

Data	
Location	Antwerp
From	2012-07-10 09:49:21 CEST
Until	2012-07-10 12:38:06 CEST
Minimum Longitude	4.403
Minimum Latitude	51.204
Maximum Longitude	4.424
Maximum Latitude	51.221
Area	2.6 km^2
Measurements	
Number of Measurements	1160
Number of Measurements with geo-coordinates from ip	0
Number of Measurements with tags	115
Number of Measurements with perceptions	138
Number of Measurements from Android products	245
Number of Measurements from Apple products	915
Coverage	
Overall duration of measurements	1:38:55
Area coverage (radius 10m)	0.20 km^2
Area coverage (radius 10m)	7.45 %
WideNoise Ids	
Number of WideNoise ids	11
Number of WideNoise ids with geo-coordinates from ip	0
Number of WideNoise ids with tags	10
Number of WideNoise ids with perceptions	11
Number of WideNoise ids from Android products	5
Number of WideNoise ids from Apple products	6
Decibel Statistics	
Average	66.36
StD	10.03
Minimum	25.61
Maximum	94.30

Table 2.9: Worldwide WideNoise Summary.

The table also covers statistics concerning WideNoise ids. There were not many users but nearly all of them tagged and added perceptions. Finally, the table aggregates the measurements and presents certain statistics on the average decibel (dB) values of the measurements (see Section 2.3.3). Comparing with Table 2.3 and already observed in Figure 2.6 the average is slightly higher and the standard deviation is lower. Again this can be explained by the fact that measurements are taken in a city (as compared to everywhere) and concentrated on a relatively small area.

Figure 2.28 shows several of the statistics from Table 2.9 as pie charts. Figure 2.28(a) shows the relative amounts of measurement durations. Figure 2.28(b) shows the relative amounts of measurements with attached tags, with perceptions, with none of those two attachments and with both. The possibility to extend durations as well as the perception dialog was not used as often as in the overall distribution. This can be explained by the fact that the users had to make many measurements in a relatively small amount of time, thus, focusing on taking the noise measurement and not on tagging or perceptions. Finally, Figure 2.28(c) shows the relative amount of measurements made by Apple products against the measurements made by Android devices. The amount of Android phones was rather high, hence the high number of Android measurements.

To illustrate how user activity is distributed, Figure 2.29 shows two log-log plots of the users sorted by frequency descending on the x-axis. For Figure 2.29(a) the number of measurements for each user is directly plotted to the y-axis. For Figure 2.29(b) the frequencies for the user as well as all preceding users frequencies are summed up.

Figure 2.30 provides a histogram with 10 dB sized bins summarizing the overall distribution of decibel values. Compared to Figure 2.20 the bins in the lower dB intervals are smaller relative to the bins in the 60 dB area. Just like the higher average dB value this indicates that cities are louder

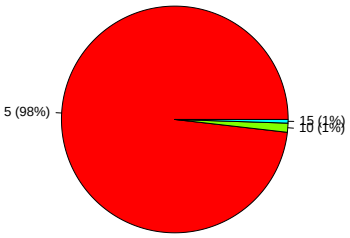

(a) Measurement durations for the Antwerp data.

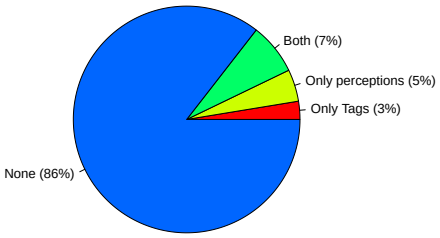

(b) Measurements with either tags, a perceptions, none, or both for Antwerp data.

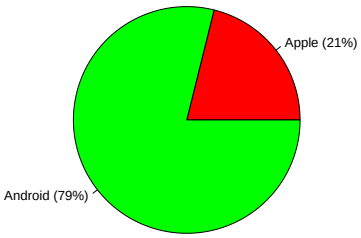

(c) Measurements from Apple and Android products for the Antwerp data.

Figure 2.28: Pie charts summarizing several statistics for the Antwerp noise measurements.

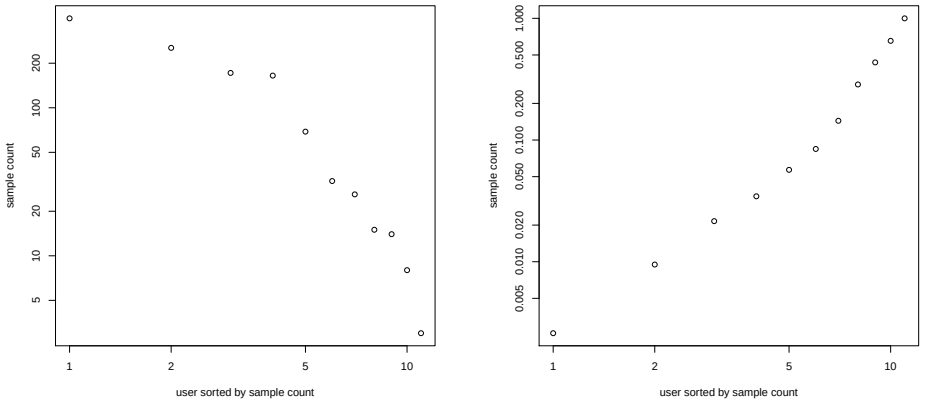

(a) Measurements per user using a log-log plot. (b) Measurements per user smoothed by summing up the frequencies per user.

Figure 2.29: Measurements per user for the Antwerp data.

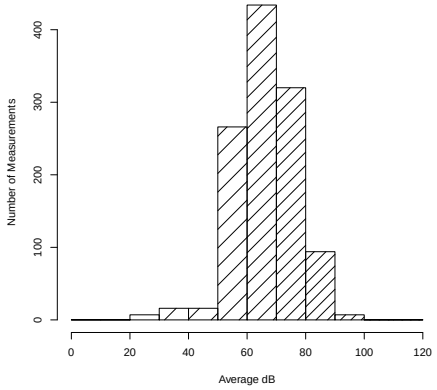

Figure 2.30: Noise Histogram for the Antwerp data.

than when considering the overall dB distribution. Also note how the covered area shows a wider spectrum of noise values than Rome (see Figure 2.26).

A list of top ten tags by count are shown in Table 2.7.

As in Table 2.5 the perceptions for Rome are listed in Table 2.11.

Finally figure 2.31 shows snapshots of the WideNoise map as available on the case study homepage[9]. The map summarizes the measurements by depicting clusters. For details on the colors coding see Section 2.3.3.

Large Scale Case Study - Heathrow

Given the time required to engage participants, work towards the large scale case studies forming part of the EveryAware project has commenced, and preliminary results in terms of data coverage are reported here. On the 19th of June, 2012, UCL started a noise monitoring campaign around London Heathrow airport, focused on the community of Isleworth which lies under the flight path(s). In this campaign we sought to engage local citizens to use WideNoise to measure noise in their

[9] `http://cs.everyaware.eu/event/widenoise/map`

Tag	Count
street	33
cars	23
bus	21
outdoor	18
traffic	11
train station	10
car	8
bus stop	7
construction work	7
traffic light	6

Table 2.10: Top ten tags by count for the Antwerp data.

Perception	Overall Average	Amount (non 0.5)	Average (excluding 0.5)
Love / Hate	0.53	100	0.62
Calm / Hectic	0.53	98	0.67
Alone / Social	0.50	96	0.67
Nature / Man-Made	0.59	128	0.83

Table 2.11: Perceptions for the Antwerp data.

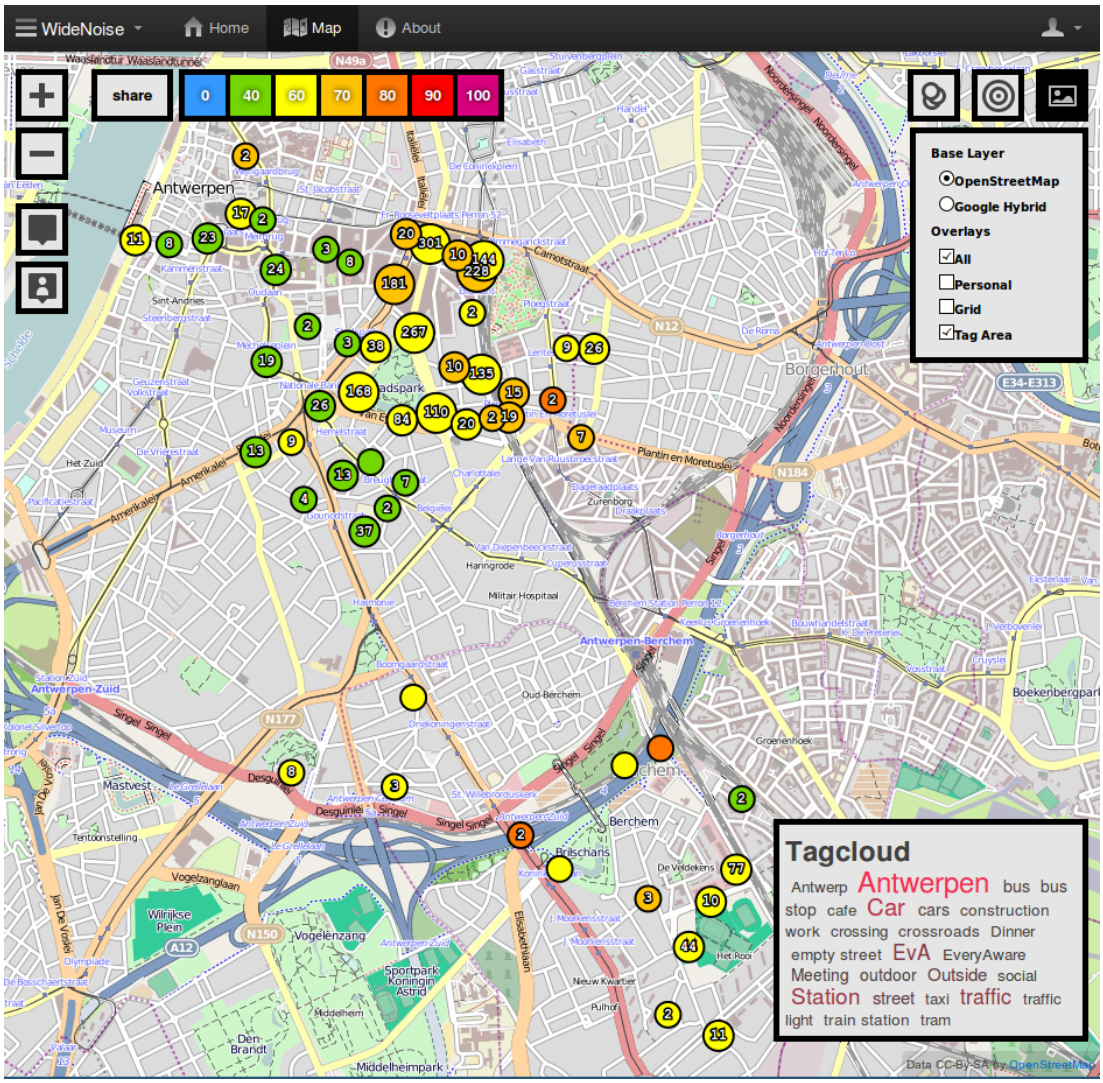

Figure 2.31: WideNoise map showing clusters.

daily environment – in which many claim to suffer from excessive noise caused by the take-off and landing operations. The purpose of this campaign, in the context of the project, was to conduct an end-to-end test of the platform formed by WideNoise and the EveryAware back-end.

To bootstrap the campaign 9 smartphones[10] were lent to community members. Other interested citizens were urged to download and install WideNoise on their own devices. To boost recruitment we ran an online and offline publicity campaign and successfully sought media attention [BBC News London, 2012]. On July 24, after 4 weeks, 7 devices[11] were reclaimed, the others remain with community members. Many people also continue to use their own devices. Therefore we consider this campaign to be an on-going effort. More details about this campaign and related coaching efforts can be found in deliverables 3.1 and 6.1.

Rather than selecting measurements taken by specific users (or devices) we have opted to extract the Heathrow dataset from the worldwide WideNoise dataset (see 2.3.3) by means of a spatio-temporal query. We delineated an area of 169 km^2 around (and including) Heathrow airport. Besides Isleworth this area also covers numerous other communities that are affected by the Heathrow flight paths. Measurements *with* geo-coordinates that lie within the boundaries of this area *and* were taken on or after 2012-06-19 are attributed to the Heathrow campaign. Consequently we are *not* considering measurements without geo-coordinates because we have no way of telling whether they were taken in the area of interest[12].

The currently (up to 2012-08-13) collected noise data consists of 3007 measurements submitted by 284 different devices/users. Interestingly, however, we have only had direct contact with about 20 inhabitants of Isleworth. The other contributors were recruited through word-of-mouth and the publicity campaign. To date, we have refrained from imposing or suggesting a systematic data collection protocol. This is because, as this large-scale case study is formed of two groups of participants from different villages, we therefore have the opportunity to investigate whether better data coverage will be obtained by providing general usage guidelines ('capture noise measurements outside') which perhaps do not impact users' daily lives and routines, or by expecting significant commitment on the part of the users and issuing more specific 'measure at this time/place' instructions. Another reason is the difficulty of coordinating participant's actions when the majority of them could only be reached through one-way (and often online) communication alone.

In terms of the data collection schemes discussed in 2.1.3, many contributors seem to have followed a stationary or semi-stationary pattern[13]. Often these people measured the passage of airplanes, typically with the intention to capture the moment the plane is overhead and thus causes the loudest noise. We know this from communications with a subset of the contributors, which are summarised in deliverable 6.3. In terms of the data collection goals discussed in 2.1.2 this type of usage can be seen as event-based measurement, possibly in combination with personal exposure measurement. Even though there was little or no coordination among contributors, nor continuous measurement, we consider this targeted data collection, driven by the motivation to collect evidence on harmful aircraft noise. This usage clearly does not result in wide spatial coverage but rather in a limited number of fairly dense clusters.

Table 2.12 summarizes the currently collected data. The coverage in space and time is given as well as statistics about tag usage, perception ratings and the smartphone platforms that have been used. We also list the duration (5, 10 or 15 s) of the measurements. This shows that most users use the default duration of 5 s. But the majority of those that extend the duration do so twice (to 15 s). Figure 2.32 illustrates some these statistics using pie charts: Figure 2.32(a) shows the relative amounts of measurements with attached tags, perception ratings, both or none; Figure 2.32(b) shows the duration of the measurements; finally, Figure 2.32(c) shows the relative amount

[10] 8 HTC Explorers and 1 Apple iPhone 3G.

[11] All of them HTC Explorers, so 1 Explorer and 1 iPhone remain in the field.

[12] There was no point in including measurements without geo-coordinates taken by users/devices that *have* submitted measurements taken around Heathrow because there were only 2 such measurements in the database.

[13] Albeit without continuous measurement because WideNoise does not support that.

of measurements made by Apple products against those made by smartphones running Android.

Data	
Location	Around Heathrow airport
From	2012-06-19
Until	2012-08-13 (on-going)
Coverage	
Area (outer bounds)[14]	130 km^2
Area (10m radius around each sample)	0.28 km^2
Time (30s before and after each sample)	52:50:16
Measurements	
Number of measurements[15]	3007 ($\pm$96 %)
Number of measurements with tags	1097 ($\pm$36 %)
Number of measurements with perception ratings	2173 ($\pm$72 %)
Number of measurements by Apple products	1723 ($\pm$57 %)
Number of measurements by Android products	1284 ($\pm$43 %)
Durations:	
○ 5 s	1766 ($\pm$59 %)
○ 10 s	448 ($\pm$15 %)
○ 15 s	793 ($\pm$26 %)
WideNoise Ids (devices[16])	
Number of WideNoise ids	284
Number of WideNoise ids corresponding to registered users	32 ($\pm$11 %)
Number of WideNoise ids with tags	46 ($\pm$16 %)
Number of WideNoise ids with perception ratings	179 ($\pm$63 %)
Number of WideNoise ids from Apple products	214 ($\pm$75 %)
Number of WideNoise ids from Android products	71 ($\pm$25 %)
Decibel Statistics	
Average	73.82
Standard deviation	10.64
Minimum	0
Maximum	102.62

Table 2.12: Summary of the on-going WideNoise campaign around Heathrow airport

Table 2.12 also covers statistics concerning WideNoise Ids addressing questions similar to the single measurement statistics: How many users tag? How many users provide perception ratings? Which smartphone platforms do they use? We should note that WideNoise Ids in fact represent devices rather than users – except when the user has registered an account. In some cases however, particularly where phones were loaned from the project, there may be instances where an individual device has been used by more than one contributor. It is assumed that these cases are rare and as such we consider each Id to represent an individual user.

Finally the table lists statistics on the sound pressure level (SPL) values that were measured (expressed in dB). We should note that, as discussed in deliverable 1.1, there is a significant error margin due to fact that WideNoise cannot be calibrated to account for the microphone sensitivity of different mobile phones. The minimum of 0 dB is an unrealistically low value which is likely caused by a hardware or low-level software malfunction that occurred during a few measurements. In the future it may be advisable to simply ignore measurements below $\pm$30 dB. The charts in Figure 2.33 summarize the overall distribution of decibel values measured during the campaign.

As was to be expected from related work [Stevens, 2012, p. 131–136], there are large differences in the efforts of the contributing citizens. To illustrate this Figure 2.34 plots the number of users that have contributed certain numbers of measurements. It is interesting to note that the 10 most active users ($\pm$3 % of the total) are together responsible for about 60 % of the measurements.

A list of top 30 tags by count are listed in Table 2.13. Clearly the vast majority of tags are related to air traffic to or from Heathrow airport.

[14] Computed as the convex hull.

[15] All *with* geo-coordinates.

[16] Each WideNoise Id represents a unique device, typically used by a single person.

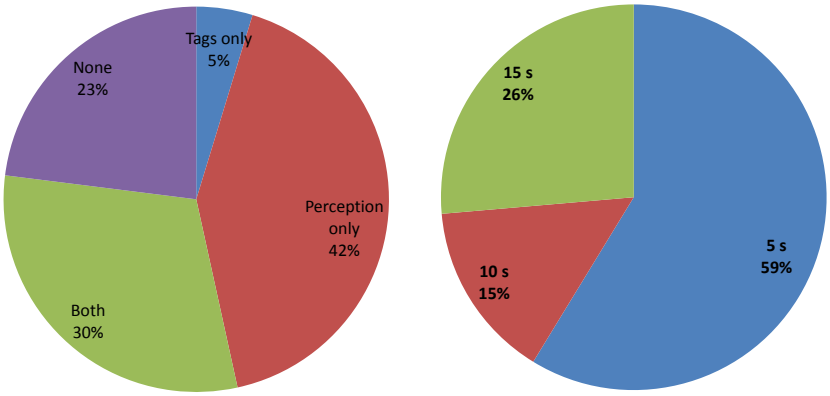

(a) Measurements with either tags, perception ratings, none, or both

(b) Measurement duration

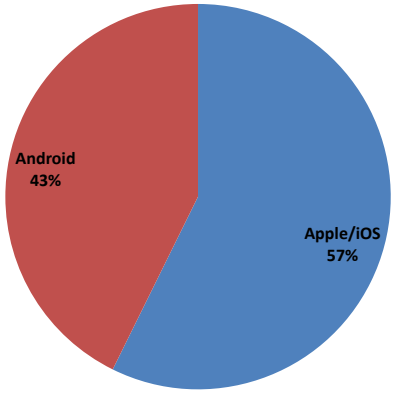

(c) Smartphone platforms: iOS vs. Android

Figure 2.32: Pie charts for measurements taken during the Heathrow campaign

The WideNoise app also asks the user to rate his/her perception of the soundscape by means of 4 sliders, each representing a different aspect. Each perception value ranges from 0 to 1, 0.5 being the neutral answer. The results are summarized in Table 2.14 and Figure 2.35. Due to the way WideNoise is designed it is unfortunately not possible to differentiate between situations where the user felt neutral a perception aspect, and situations where he/she did not feel like answering the question (and thus left the slider untouched): in both cases the result is a perception value of 0.5. However, looking at the peaks in 2.35 it is very likely that in the majority of cases 0.5 should be interpreted as the result of the second situation – i.e. the perception rating step was essentially skipped[17]. Therefore Table 2.14 lists averages with and without 0.5 answers taken into account.

Figure 2.36 shows a screenshot of the WideNoise map for the area of study[18]. The map summarizes the measurements by clustering them. Finally Figure 2.37 shows a map in which the measurements are aggregated and averaged in a regular grid with cells of 500 m $\times$ 500 m.

[17] In Table 2.12 & Figure 2.32(a) we consider measurements with 0.5 on all 4 aspects to be lacking perception ratings.

[18] The dynamic cluster map can be explored at:
`http://cs.everyaware.eu/event/widenoise/map?lon=-0.3869&lat=51.4728&zoom=13`.

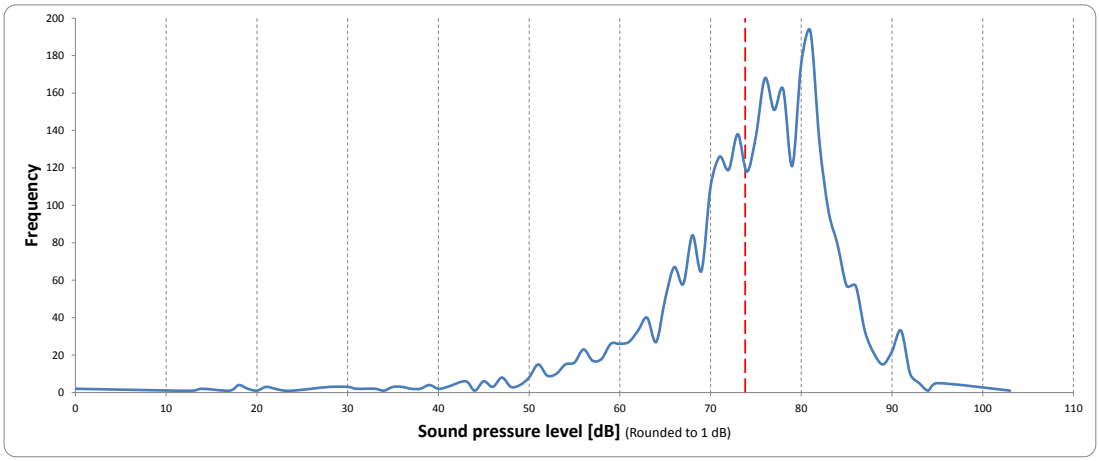

(a) Distribution curve, measurements rounded to 1 dB (average level is indicated in red)

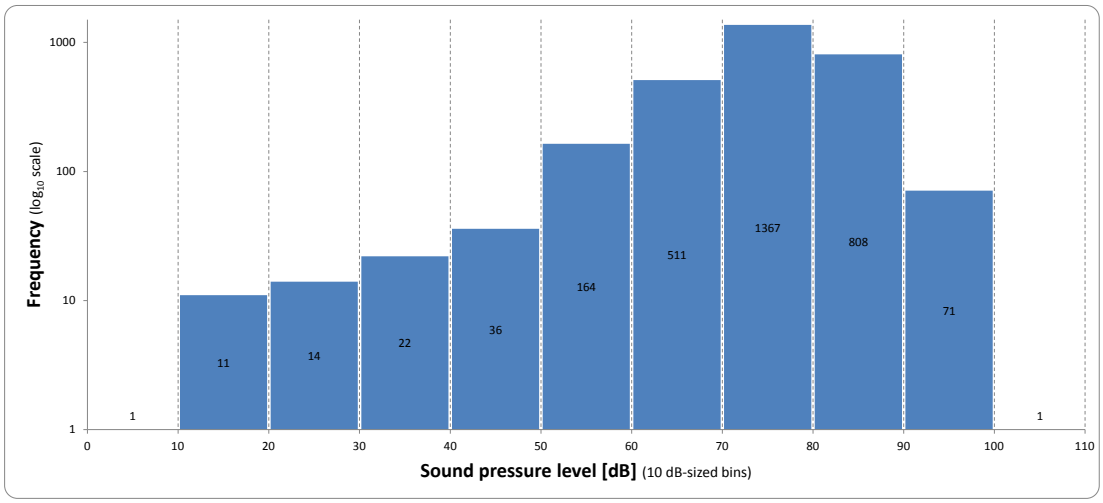

(b) Histogram with 10 dB bins

Figure 2.33: Distribution of sound pressure level measurements during the Heathrow campaign.

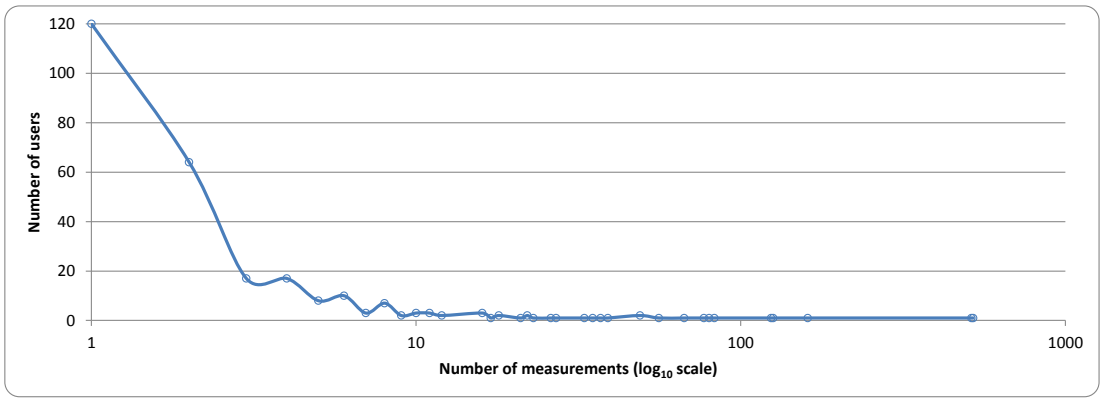

Figure 2.34: Number of users with certain number of measurements.

Tag	Count	Note
garden	500	
plane	268	
street	78	
aircraft	63	
south runway	44	
background	42	
noisy	33	
north runway	31	
back garden	23	Also counted as "garden"
big plane	20	Also counted as "plane"
heathrow	18	
small plane	15	Also counted as "plane"
airplane	15	
twickenham rd	14	
distant plane	12	
train	12	
middle of college road	11	
balcony	9	
plane heard from inside double glazing	9	Also counted as "plane"
traffic	9	
front of house	8	
car	8	
quiet sunday	7	
walking through park	5	
coming in on both runways	4	
747	4	
inside home aircraft noise	4	
river	4	
bus	3	
wrongrunway	3	

Table 2.13: Top 30 tags by count.

Perception	Overall Average	Amount (non 0.5)	Average (excluding 0.5)
Love / Hate	0.65	1147 (±38 %)	0.89
Calm / Hectic	0.59	936 (±31 %)	0.80
Alone / Social	0.44	773 (±26 %)	0.28
Nature / Man-Made	0.81	2003 (±67 %)	0.97

Table 2.14: Summary of the perception ratings given in the campaign around Heathrow

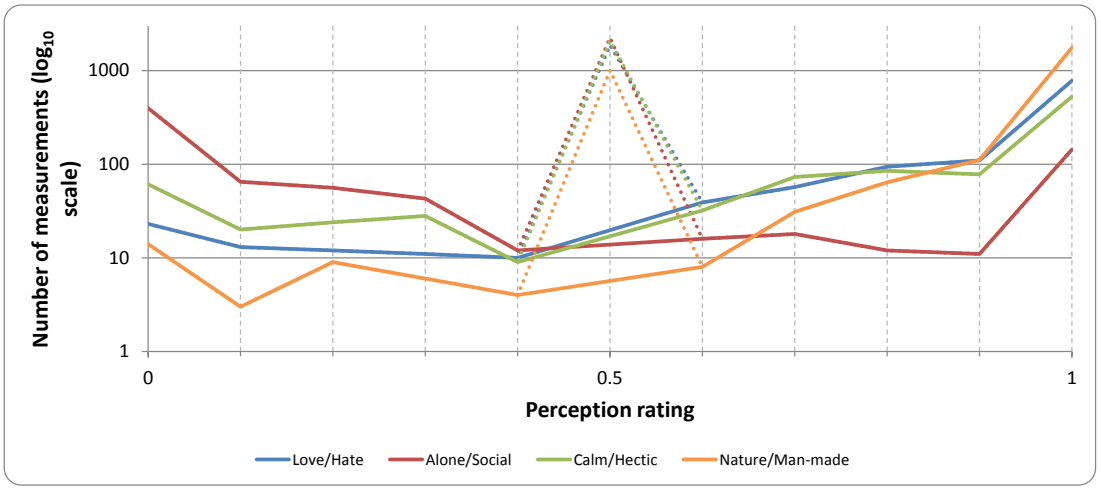

Figure 2.35: Distribution of the perception ratings given in the campaign around Heathrow

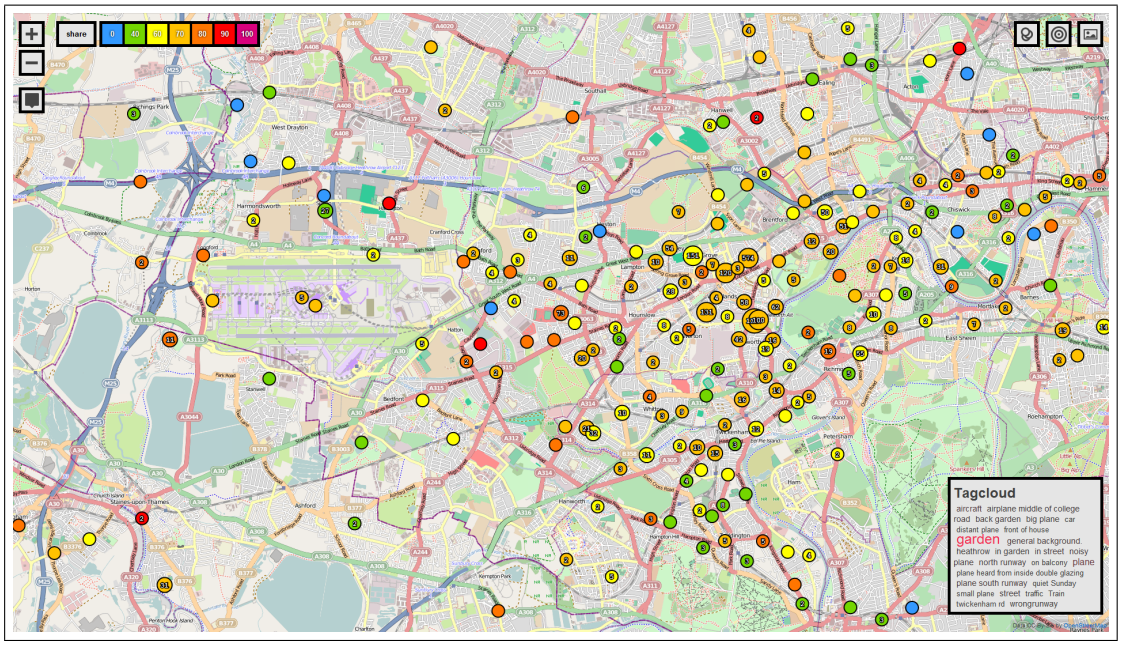

Figure 2.36: WideNoise map for the area around Heathrow (clustered measurements).

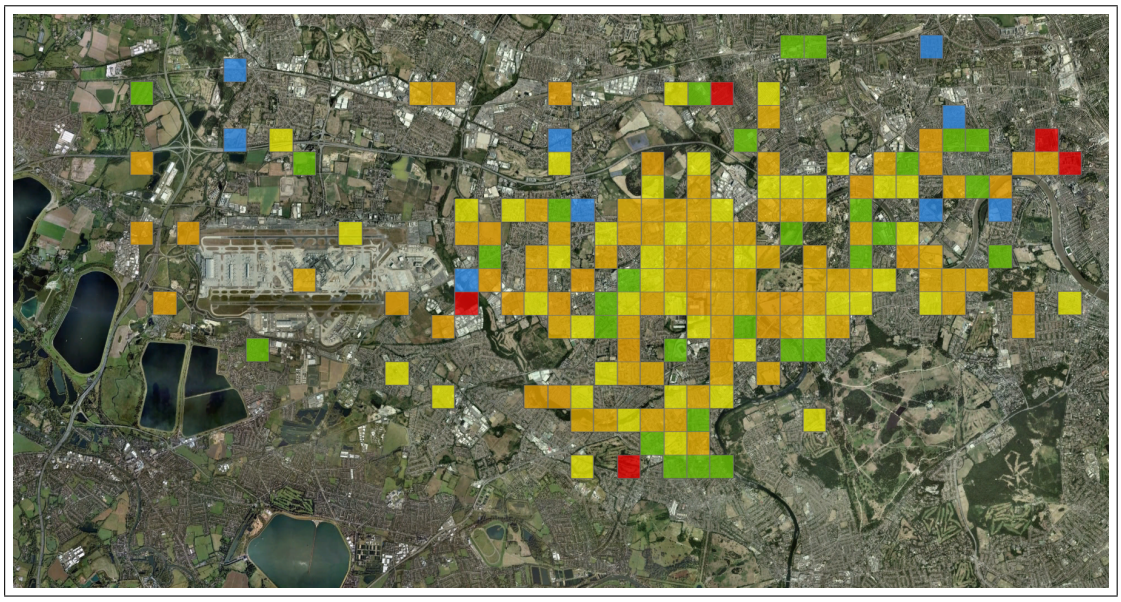

Figure 2.37: Grid-based map for the area around Heathrow.

2.3.4 Conclusions for set-up of case studies: noise

The results of the large case study at Heathrow demonstrate that uncoordinated sensing across an area this large does not lead to dense spatial and temporal coverage. Reaching dense coverage without coordination would require massively more contributors, which may not be attainable in the short term. An alternative approach is to foster collaboration between smaller groups of highly motivated contributors that live close to one another. By coordinating the actions of such groups it is possible to achieve dense spatio-temporal coverage, albeit for much smaller areas. Such an approach has been successfully demonstrated by [D'Hondt et al., 2011; Ellul et al., 2011; Francis et al., 2008; Stevens, 2012].

Therefore we consider it advisable to move towards a more coordinated, goal-driven approach in future case studies of urban noise conducted in the scope of the EveryAware project. By devising targeted data collection protocols – specifying where, when and for how long contributors should measure – in collaboration with committed contributors we can aim to answer specific questions voiced by the citizens[19]. This approach could increase motivation and commitment and thereby result it better spatio-temporal coverage – at least for the chosen times and places – than is feasible without such coordination. Of course these case studies can happen alongside uncoordinated worldwide WideNoise usage.

[19] E.g. What is the average peak exposure caused by overhead flights? Are regulations on night flights respected? Are flight of airline X consistently louder than those of airline Y? Is there a difference in the average sound level in street A vs. street B? Is there a difference between summer and winter? Etc.

Chapter 3

Interpolation tools

The use of interpolation techniques is required to estimate air quality or noise at locations where measurements are lacking. A multitude of (geostatistical) interpolation techniques have been developed (summary from [Akkala et al., 2010]):

- Nearest Neighbour
- Triangulated irregular network
- Polynomial regression
- Global polynomial interpolation
- Local polynomial interpolation
- Trend surface analysis
- Inverse distance weighting (IDW)
- Splines
- Kriging
- Radial basis functions
- Artificial neural networks

A selection of these methods will be tested for application in EveryAware. These tests will be performed on EveryAware data that will be acquired in future test cases. Awaiting these event, a brief overview of techinques is given and their applications in the air quality and noise literature are highlighted.

3.1 Review of techniques

- Nearest neighbour interpolation is a simple interpolation technique by which the value of a parameter at a non-given location is estimated as the parameter value at the nearest (e.g. lowest Euclidean distance) location. Nearest neighbour does not consider the value of neighbouring points, and yields a piecewise-constant interpolant.
- The triangulated irregular network (TIN) model represents a surface as a set of contiguous, non-overlapping triangles. Within each triangle the surface is represented by a plane. The triangles are made from a set of points called mass points. A TIN is typically based on Delaunay triangulation on a selection of mass points which are most necessary to an accurate representation.

- Polynomial regression interpolation fits the parameter of interest as high order bivariate polynomial function of regressor variables (latitude, longitude). The value of a parameter at location i (latitude$_i$, longitude$_i$) is estimated by the polynomial function. Global polynomial interpolation makes use of one polynomial function to cover the entire study area, whereas local polynomial interpolation fits many different polynomial functions, each of which is optimized for a neighbourhood.
- Trend surface analysis
- Inverse distance weighting (IDW) is an interpolation technique that assigns a value to unknown points based on a weighted average of scattered known points. The weighting function is a function of the distance between the unknown point and known points, and can take various forms [Shepard, 1968].
- Splines interpolation fits piecewise polynomial functions (most often cubic) through the data as a continuous surface. At unknown locations, the spline fit gives an interpolated value.
- Kriging methods are known as optimal interpolators because they supply the best linear unbiased estimate of a variable's value at any point in the study area. Kriging methods exploit the spatial dependence in the data. The major advantage of Kriging over other methods is that kriging supplies standard errors (kriging variance) at any unsampled location in the study area.
- Artificial neural networks are highly flexible information processing paradigms that are inspired by the way biological nervous systems. The information processing system is composed of a large number of highly interconnected processing elements (neurones) working in unison to solve specific problems. ANNs learn by example through a learning process.

3.2 Interpolation methods for air quality: literature review

A literature review on the use of nearest neighbour interpolation techniques for air quality (based on Web of Science searches using (1) nearest neighbour and air and (pollution or quality), and (2) spatial and interpolation and nearest and air and (pollution or quality) as search terms) yielded a small amount of results. Basically, two types of applications were found in the literature. A first group of studies (2) used nearest neighbour interpolation to fill missing data into air quality time series and to predict air quality time series. [Junninen et al., 2004] observed a reasonable performance of NN interpolation to fill missing values, depending on the size of the data gap and the parameter under investigation. Self organizing maps and multi-layer perceptron models performed slightly better than NN, however, the computational power requirements of NN was much less. [Gautam et al., 2008] propose a methodology to predict chaotic air quality time series (ozone concentration) based on artificial neural networks coupled to a nearest neighbour search algorithm. [Martin et al., 2008] apply k-Nearest Neighbours (k-NN) classifiers in order to predict future peaks of carbon monoxide. [Shao et al., 2007] used a NN for interpolation of the output from multi-scale air quality models from coarse resolution to fine resolution, and showed that bilinear interpolation generally gains better results.

Another group of studies used NN interpolation to compute a map of pollutant concentrations which were then used to assess the individual exposure to air pollution. In these studies, exposure is determined by data from the nearest monitor. Most often, these results are further compared with exposures derived from more complex interpolation methods. [Bell, 2006], for example, made exposure estimates that were generated for a case study high ozone episode in the Northern Georgia Region of the U.S. based on measurements and concentration estimates from an air quality modelling system. Results based on concentration fields from the air quality modelling system revealed

Table 3.1: Summary of interpolation methods and their applications (adopted from [Akkala et al., 2010])

	Interpolation technique	Principle	Advantage	Disadvantage	Best-suited scenario
1	Nearest neighbour (NN) and Thiessen polygons	selection of the value at closest data point	ease of use	inaccuate in less densely sampled scenarios	densely sampled data
2	Triangulated irregular network (TIN)	set of conterminous triangles associated with a mass factor used to define the space	ability to describe the surface at different levels of resolution	requires visual inspection and manual control of the network	dense and moderate distribution of data points
3	Polynomial regression (PR)	fits the variable of interest to a linear combination of regressor variables	simple model	poor ability to predict outside the range of data points	moderately dense sampling with regard to global variation
4	Global polynomial interpolation (GPI)	works by capturing coarse-scale patterns in the data, and fitting a polynomial	computationally less expensive	estimation errors increase exponentially with increasing complexity	regions having sparse data points and simple data patterns
5	Local polynomial interpolation (LPI)	similar to GPI, but curve is fitted to a local subset defined by a window	can incorporate short range variations	misses the global trends in the data	well-distributed data points, preferably with local data patterns
6	Trend surface analysis (TSA)	separates the data into regional and local variations	assists in removal of broader trends prior to further analysis	edge effects and multicollinearity caused by spatial autocorrelation	regions having well-distributed data with important local trends, and not so important global trends
7	Inverse distance weighting (IDW)	linear combination of known points, weighted inversely by distance	ease to use and works with noisy data	spatial arrangement of samples does not affect weights	moderately dense sampling with regard to local variation
8	Splines	fits a smooth curve to a series of data points	visually appealing curves or contour lines	may mask uncertainty in the data	irregularly-spaced data
9	Kriging	similar to the principle of IDW, however additionally accounts for the spatial arrangement	best linear unbiased spatial predictor, no edge effects	sophisticated programming required and problems with non-stationarity in real-world data sets	well-distributed data with no discontinuities
10	Radial basis functions (RBF)	similar to the principle of splines, except the curve is not smooth	requires fewer samples	requires good coverage of the input space and is not suited for extrapolation	regions with well-distributed data points, through space
11	Artificial neural networks (ANN)	learn complex patterns in the available data using (sigmoid) functions	ability to learn and generalize data, works well with sparse data distributions, extrapolation capability	risk of poor interpolation caused by over-learning or under-earning	regions ranging from sparse irregularly distributed data to well-distributed data

spatial heterogeneity that was obscured by approaches based on the monitoring network (nearest monitor interpolation). Monitoring data alone was shown to be insufficient to estimate exposure for certain areas, especially for rural populations. [Kim et al., 2009] compared nearest monitoring and kriging interpolation for exposure predictions and assessed how both methods affect relative risk estimates for cardiovascular events in a single geographic area. The authors concluded that, when the underlying exposure distribution has a large amount of spatial dependence, both kriging and nearest-monitor predictions gave good health effect estimates. For exposure with little spatial dependence, kriging exposure was preferable but gave very uncertain estimates. [Son et al., 2010] compared several interpolation methods to estimate individual-level exposures to air pollution from ambient monitors for several air pollutants. Findings suggested that spatial interpolation methods may provide better estimates than nearest monitoring values alone by reflecting the spatial variability of individual-level exposures and generating estimates for locations without monitors.

Triangulated irregular network is not implemented for air quality interpolation. A search (triangulated irregular network and air and quality) did not give any record. Also polynomial regression and trend surface techniques are, to our knowledge, not used for spatial interpolation of air quality measurements.

The most common technique used in the air pollution field is Kriging. Kriging methods are used for the real-time and historic assessment of the ambient air quality. The model RIO, for example, is an interpolation model that can be classified as a detrended Kriging model [Janssen et al., 2008]. In a first step, the local character of the air pollution sampling values is removed in a detrending procedure. Subsequently, the site-independent data is interpolated by an Ordinary Kriging scheme to a country-wide 5 by 5 km grid. Finally, in a re-trending step, a local bias is added to the Kriging interpolation results. A non-exhaustive overview of studies that used Kriging for the spatial interpolation of air quality parameters are given in Table 3.2.

Artificial neural networks have been used to forecast ozone and PM10 concentrations in an urban area [Carnevale et al., 2011]. Here, artificial neural networks are applied to get point-wise forecasting. In the second step, the forecasts obtained at the monitoring station locations are spatially interpolated all over the domain using the cokriging technique. [Pfeiffer et al., 2009] proposed a new method to calculate the average spatial distribution of air pollutants based on diffusive sampling measurements and artificial neural networks. The best fit could be achieved with an emissions inventory including previously simulated concentration plumes and population density data as input nodes for the neural network, resulting in realistic maps of the annual average distribution of NO(2) in Cyprus using a 1 x 1 km grid. More examples of the use of ANN for spatial interpolation of pollutant concentrations were not found. Recently, interpolation of air quality shifted toward the so called land use regression models (LUR models). LUR models encompass a diverse group of models that use additional covariates in addition the geospatial information to interpolate air quality at unknown locations. The modelling core of LUR models is often a regression, but ANN have also been applied in this context. Currently, most LUR models are implemented at a lower spatial and temporal resolution (e.g. monthly or yearly averaged concentrations on a 1 by 1 km grid) and their performance at high resolution remains unclear.

In conclusion, the most commonly used techniques are nearest neighbour, kriging and artificial neural networks within land use regression models. In the majority of the applications the spatial and temporal resolution of air quality maps is low (e.g. yearly averages on a 1 km grid) in comparison to the data that are obtained in EveryAware. The potential of statistical models and interpolation tools on a high resolution dataset is therefore questionable. Also the highly dynamic behaviour of pollutants in an urban environment and the fact that the urban outdoor environment largely consists of discontinuous line elements, interferes with the application of the described interpolation methods.

Table 3.2: Literature review: Kriging for air quality interpolation.

Reference	Location	Pollutant	Spatial coverage	Spatial resolution	Temporal coverage	Temporal resolution
[Janssen et al., 2008]	Belgium	O_3, SO_2, NO_2, PM10	Belgium	5 by 5 km		daily average
[Tayanc, 2000]	Istanbul, Turkey	SO_2, PM	Istanbul	?	1985?91	monthly average
[Leem et al., 2006]	Incheon, Republic of Korea	SO_2, NO_2, CO, PM_{10}	metropolitan area of Incheon	0.170 km grid	April 2000 – December 2002	monthly average
[Mulholland et al., 1998]	Atlanta, USA	O_3	Atlanta MSA, 50 miles in each direction	3 by 3 km	1993-95	max. 1h and 8h average, daily
[Bell, 2006]	Georgia, USA	O_3 Northern Georgia, USA	4 by 4 km grid	August 15, hour 00 to August 18, hour 00 1995	hourly average	
[Liu and Rossini, 1996]	Toronto, Canada	O_3	Toronto metropolitan area	?	June – August 1992	12h average
[Denby et al., 2008]	Europe	PM10	Europe	25 km grid	2003	annual mean
[Duc et al., 2000]	Sydney, Australia	NO_x, O_3 Sydney	?	1993 to 1994	monthly average of daily maximum	
[Whitworth et al., 2011]	Harris county, Texas	benzene	Harris county	?	1999	annual average of 24-h concentration

3.3 Interpolation methods for noise measurements: literature review

In stark contrast to air quality, there is surprisingly little literature about the use of interpolation methods for (urban) noise, in particular when measured using the crowd-sourcing approach proposed by the EveryAware project. The few studies that do mention interpolation methods in this context do not justify the choice for a particular one. For instance [Tsai et al., 2009] and [Akgüngör and Demirel, 2008] use Kriging to interpolate measurements of urban noise but neither substantiate this choice, nor considers alternatives. [Abdurrahman and Bostanci, 2012] employ IDW, Kriging, and Radial basis functions, but although they note that the choice of method significantly affects the results they do not indicate which method was deemed most suitable. As far as we know there is no established method for interpolation of noise measurements.

More generally we should note that, due to the central shared assumption of a continuous surface [de Smith et al., 2009, Chapter 6], generic interpolations methods are not that suitable for interpolation urban noise across large areas, due to the limited spatial and temporal reach (see 2.3.2) and the effect of obstacles such as buildings. Instead it is likely that better results could be achieved if a noise-specific interpolation method (one that accounts for the physical propagation of sound) were devised, instead of relying on a generic methods.

In earlier citizen science studies of urban noise [Ellul et al., 2011; Francis et al., 2008; Stevens, 2012] measurements where aggregated and averaged in cells of a regular grid, instead of using an interpolation method across a wider area. This means the area of study is divided by a grid with cells of equal size (e.g. with cells of 20×20 m). Then each individual measurement is assigned to a cell based on its geographical co-ordinates. Statistics such as average, standard deviation, minima and maxima can then be computed for the data in each cell. Finally a map is generated representing the average sound level measured in each cell. An example of such a map is shown in Figure 2.37. One of the factors that needs to be take into account when deciding on a suitable size for the grid cells is the inherent error on geographical co-ordinates obtained from GPS. Such errors tend to vary with the time of day (due to GPS satellite positions), atmospheric conditions, and especially the density and height of nearby buildings [Stevens, 2012].

In the context of strategic noise mapping (typically based on predictions rather than measurements) interpolation methods commonly play a role. However, as noted by [Murphy and King, 2010; Murphy et al., 2006], different software packages use different interpolation methods and hence lead to different results (making maps of different cities hard to compare). Therefore the authors stress that clear instructions on which interpolation method(s) must be used ought to be incorporated in the END [European Parliament and Council, 2002], or supporting publications – which now leave the choice to the local authorities responsible for the creation of the maps[1].

[1] A task that is commonly subcontracted to specialised firms.

Chapter 4

Conclusions and Perspectives

In EveryAware, data coverage is defined in two domains: (1) temporal coverage and (2) spatial coverage. Basically, one sensor datum is acquired on a certain location in space and time. Combining these data leads to a temporal and/or spatial representation of reality. The representativity of this representation is directly linked to the temporal and spatial data coverage, where a higher data coverage leads to a better representation.

Two environmental parameters are examined in the EveryAware project: (1) air pollution and (2) noise pollution. Both pollutants are highly dynamic, resulting in a high variability of air quality and noise levels, both in space and time. Examples were shown to illustrate the spatio-temporal variability of air quality and noise. Within this setting, the EveryAware test cases will be set up to quantify the air quality and noise levels in urban environments. From the pilot campaigns it was observed that the data coverage needed to characterize the air quality and noise level requires repeated measurements along the spatial and temporal dimensions. To satisfy the need of repeated measurements, several types of data collection are defined. Opportunistic data collection is distinguished from data collection, the latter referring to a deliberately planned collection strategy, and stationary data collection is distinguished from mobile data collection. The devices to collect environmental data ,i.e. the SensorBox and the WideNoise smartphone application, allow to perform these different data collection modes. However, the SensorBox is continuously measuring during a period of time at a temporal resolution of 1 second, whereas the Widenoise application is used in a more discontinuous way. Moreover, the number of citizens carrying the SensorBoxes is rather limited compared to the number that has access to WideNoise, and the use of WideNoise is likely to be more easy. The different operational modes of both devices require a different approach to fulfil the data coverage needs.

Several test cases were deployed. From these campaigns it was observed that a quite high data coverage could be obtained in the EveryAware data collection framework under certain conditions. For air quality, a mobile data collection set-up can lead to a dense monitoring of the air quality. Results showed however that – in order to get representative estimates of the air quality at street level – focus and repetition are critical. For noise, most of the test case studies were confined in space (Heathrow, Antwerp, Rome), in contrast to the worldwide application of WideNoise. From the most elaborate test campaigns, the worldwide application and the Heathrow test campaign, the participation differed a lot between citizens leading to a similar density plot of the number of measurements in function of the proportion of participants. A few participants collect a major part of the data. A big difference was found in the data perception rating between Heathrow (72%) and the worldwide application (15%), most probably due to the more direct communication with the participants in the former campaign. This example stresses the importance of direct involvement to obtain high numbers of measurements in EveryAware. In future case studies of urban noise conducted in the scope of the EveryAware project, it is advisable to move towards a more goal-driven approach. By devising targeted data collection protocols – specifying where, when and for

how long contributors should measure – in collaboration with committed contributors we can aim to answer specific questions voiced by the citizens. This approach could increase motivation and commitment and thereby result in better spatio-temporal coverage – at least for the chosen times and places – than is feasible without such coordination. Of course these case studies can happen alongside uncoordinated worldwide WideNoise usage.

In summary, the concerns voiced by citizens result in the definition of the measurement goals. In turn, the goal of the measurement campaign determines the focus of the measurement campaign (when and where are the measurements made) and the most suitable data collection scheme. The measurement goal has also a direct impact on citizen involvement and the number of volunteers that are prepared to carry out measurements. As indicated, the number of measurement devices and their operation mode affects on the number of volunteers and feasibility of the different data collection schemes. The number of volunteers, focus of the study and data collection scheme determine the spatial and temporal data coverage. On the other hand, spatio-temporal data requirements for a given measurement goal determine the number of volunteers needed and the focus of the measurements.

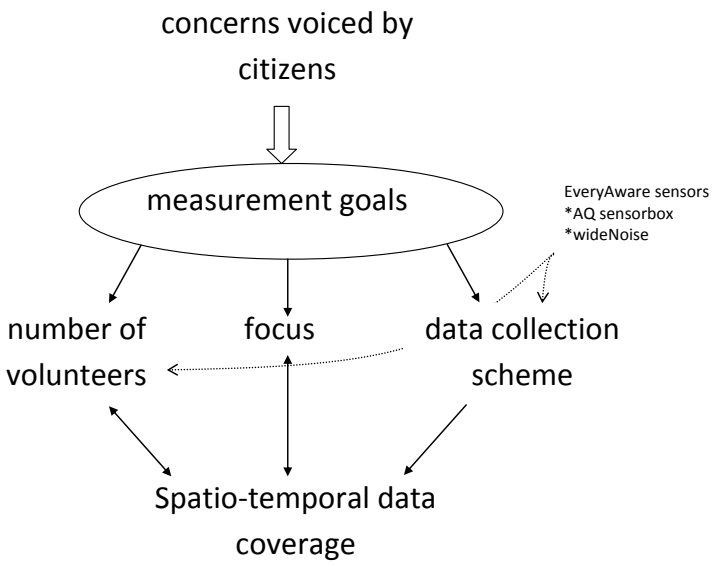

Data interpolation can be used to estimate the air quality or noise at locations where observations are lacking. Interpolation techniques establish a relationship between the air quality or noise at unknown locations and the air quality or noise at (nearby) locations. Interpolation of air quality finds its application in mapping and exposure studies. The resolution at which interpolations are made is typically much coarser than the resolution of the EveryAware data (e.g. yearly averaged concentrations interpolated on a regular 5 km grid). Their usefulness on a high resolution is questionable given the highly dynamic behaviour of air and noise pollution and the fact that the urban outdoor environment largely consists of discontinuous line elements, but was not investigated so far. Future research will assess the possibilities within the EveryAware framework.

Bibliography

G Abdurrahman and B Bostanci. Production of geographic information system aided noise maps. In *FIG Working Week 2012: Knowing to manage the territory, protect the environment, evaluate the cultural heritage (Rome, Italy, 6-10 May 2012)*, 2012. URL `http://www.fig.net/pub/fig2012/papers/ts07d/TS07D_geymen_bostanci_6116.pdf`.

AP Akgüngör and A Demirel. Investigating urban traffic based noise pollution in the city of Kirikkale, Turkey. *Transport*, 23(3):273–278, 2008. doi: 10.3846/1648-4142.2008.23.273-278.

A Akkala, V Devabhaktuni, and A Kumar. Interpolation techniques and associated software for environmental data. *Environmental Progress & Sustainable Energy*, 29(2):134–141, 2010.

BBC News London. Smartphone trial to capture heathrow flight noise, 2012. URL `http://www.bbc.co.uk/news/uk-england-london-18513299`. 2012-06-19.

ML Bell. The use of ambient air quality modeling to estimate individual and population exposure for human health research: A case study of ozone in the northern georgia region of the united states. *Environment International*, 32(5):586–593, 2006.

P Berghmans, N Bleux, L Int Panis, VK Mishra, R Torfs, and M Van Poppel. Exposure assessment of a cyclist to pm10 and ultrafine particles. *Science of the Total Environment*, 407:1286–1298, 2009.

H Boogaard, GPA Kos, EP Weijers, NAH Janssen, PH Fischer, SC van der Zee, JJ de Hartog, and G Hoek. Contrast in air pollution components between major streets and background locations: Particulate matter mass, black carbon, elemental composition, nitrogen oxide and ultrafine particle number. *Atmospheric Environment*, 45(3):650–658, 2011.

D Brugge, JL Durant, and C Rioux. Near-highway pollutants in motor vehicle exhaust: A review of epidemiologic evidence of cardiac and pulmonary health risks. *Environmetnal Health*, 6(23), 2007.

C Carnevale, G Finzi, E Pisoni, V Singh, and M Volta. An integrated air quality forecast system for a metropolitan area. *J. Environ. Monit.*, 13:3437–3447, 2011. doi: 10.1039/C1EM10303B.

LY Chan, WS Kwok, SC Lee, and CY Chan. Spatial variation of mass concentration of roadside suspended particulate matter in metropolitan hong kong. *Atmospheric Environment*, 35(18): 3167–3176, 2001.

MJ de Smith, MF Goodchild, and P Longley. *Geospatial Analysis: A Comprehensive Guide to Principles, Techniques and Software Tools*. Matador, 3 edition, 2009. ISBN 978-1848761582.

B Denby, M Schaap, A Segers, P Builtjes, and J Horalek. Comparison of two data assimilation methods for assessing pm10 exceedances on the european scale. *Atmospheric Environment*, 42(30):7122–7134, 2008.

D'Hondt, Stevens, and Jacobs. Participatory noise mapping works! Preprint. Submitted to *Pervasive and Mobile Computing*. Conditionally accepted., December 2011. URL http://www.noisetube.net/publications/partnoisemaps.pdf.

E Dons, L Int Panis, M Van Poppel, J Theunis, H Willems, R Torfs, and G Wets. Impact of time-activity patterns on personal exposure to black carbon. *Atmospheric Environment*, 45:3594–3602, 2011.

E Dons, L Int Panis, M Van Poppel, J Theunis, and G Wets. Personal exposure to black carbon in transport microenvironments. *Atmospheric Environment*, 55:392–398, 2012.

H Duc, I Shannon, and M Azzi. Spatial distribution characteristics of some air pollutants in sydney. *Mathematics and Computers in Simulation*, 54(1–3):1–21, 2000.

C Ellul, L Francis, and M Haklay. A Flexible Database-Centric Platform for Citizen Science Data Capture. In *Computing for Citizen Science Workshop (8 December 2011), held at IEEE eScience 2011, tyhe 7th IEEE e-Science conference (5-8 December 2011, Stockholm, Sweden)*, December 2011. URL http://itee.uq.edu.au/~eresearch/workshops/compcitsci2011.

European Commission. Report from the Commission to the European Parliament and the Council on the implementation of the Environmental Noise Directive in accordance with Article 11 of Directive 2002/49/EC. Report COM(2011) 321 final, June 2011. URL http://eur-lex.europa.eu/LexUriServ/LexUriServ.do?uri=CELEX:52011DC0321:EN:NOT.

European Parliament and Council. Directive 2002/49/EC of 25 June 2002 relating to the assessment and management of environmental noise. *Official Journal of the European Communities*, L 189(45):12–26, 2002. ISSN 0378-6978. URL http://ec.europa.eu/environment/noise/directive.htm.

M Florentine, NP Arthur, and RF Richard, editors. *Loudness*, volume 37 of *Springer Handbook of Auditory Research*. Springer New York, 2011. ISBN 978-1-4419-6711-4. doi: 10.1007/978-1-4419-6712-1.

L Francis, C Whitaker, and M Haklay. Noise Mapping Helps Citizens Take Action. *GIS Professional*, (23):26–28, 2008.

AK Gautam, AB Chelani, VK Jain, and S Devotta. A new scheme to predict chaotic time series of air pollutant concentrations using artificial neural network and nearest neighbor searching. *Atmospheric Environment*, 42(18):4409–4417, 2008.

L Goines and L Hagler. Noise Pollution: A Modern Plague. *Southern Medical Journal*, 100(3):287–294, March 2007. ISSN 0038-4348. doi: 10.1097/SMJ.0b013e3180318be5.

B Gomiscek, H Hauck, S Stopper, and O Preining. Spatial and temporal variations of pm1, pm2.5, pm10 and particle number concentration during the auphep-project. *Atmospheric Environment*, 38:3917–3934, 2004.

G Hagler, ED Thoma, and RW Baldauf. High-resolution mobile monitoring of carbon monoxide and ultrafine particle concentrations in a near-road environment. *J. Air & Waste Manag. Assoc.*, 60(3):328–336, 2010.

N Hudda, K Cheung, KF Moore, and C Sioutas. Inter-community variability in total particle number concentrations in the eastern los angeles air basin. *Atmospheric Chemistry and Physics*, 10(23):11385–11399, 2010.

International Electrotechnical Commission. Electroacoustics – Sound level meters – Part 1: Specifications. IEC 61672-1:2002, May 2002. URL http://webstore.iec.ch/webstore/webstore.nsf/ArtNum_PK/28763. Adopted by the European Committee for Electrotechnical Standardization (CENELEC) as EN 61672-1:2003. Mentioned page numbers refer to the EN 61672-1:2003 document.

International Organization for Standardization. Acoustics – Description, measurement and assessment of environmental noise – Part 1: Basic quantities and assessment procedures. ISO 1996-1:2003, 2003. URL http://www.iso.org/iso/catalogue_detail?csnumber=28633.

International Organization for Standardization. Acoustics – Description, measurement and assessment of environmental noise – Part 2: Determination of environmental noise levels. ISO 1996-2:2007, 2007. URL http://www.iso.org/iso/catalogue_detail?csnumber=41860.

S Janssen, G Dumont, F Fierens, and C Mensink. Spatial interpolation of air pollution measurements using corine land cover data. *Atmospheric Environment*, 42(20):4884–4903, 2008.

H Junninen, H Niska, K Tuppurainen, J Ruuskanen, and M Kolehmainen. Methods for imputation of missing values in air quality data sets. *Atmospheric Environment*, 38(18):2895–2907, 2004.

SY Kim, L Sheppard, and H Kim. Health effects of long-term air pollution influence of exposure prediction methods. *Epidemiology*, 20(3):442–450, 2009.

KM Latha and KVS Badarinath. Seasonal variations of black carbon aerosols and total aerosol mass concentrations over urban environment in india. *Atmospheric Environment*, 39(22):4129–4141, 2005.

J-H Leem, BM Kaplan, YK Shim, HR Pohl, CA Gotway, SM Bullard, JF Rogers, MM Smith, and CA Tylenda. Exposures to air pollutants during pregnancy and preterm delivery. *Environ Health Perspect*, 114(6):905–910, 2006.

P Lenschow, H-J Abraham, K Kutzner, M Lutz, J-D Preuß, and W Reichenbächer. Some ideas about the sources of pm10. *Atmospheric Environment*, 35(1):23–33, 2001.

AJ Lilienthal, M Reggente, M Trincavelli, JL Blanco, and J Gonzalez. A statistical approach to gas distribution modelling with mobile robots – the kernel dm+v algorithm. In *Proceedings of the IEEE/RSJ International Conference on Intelligent Robots and Systems (IROS)*, pages 570–576, 2009.

LJS Liu and AJ Rossini. Use of kriging models to predict 12-hour mean ozone concentrations in metropolitan toronto - a pilot study. *Environment International*, 22(6):677–692, 1996.

ML Martin, U Turias, FJ Gonzalez, PL Galindo, FJ Trujillo, and CG Puntonet. Prediction of co maximum ground level concentrations in the bay of algeciras, spain using artificial neural networks. *Chemosphere*, 70(7):1190–1195, 2008.

P Monkkonen, R Uma, D Srinivasan, IK Koponen, KEJ Lehtinen, K Hameri, R Suresh, VP Sharma, and M Kumala. Relationship and variations of aerosol number and pm10 mass concentrations in a highly polluted urban environment - new delhi, india. *Atmospheric Environment*, 38(3): 425–433, 2004.

C Monn. Exposure assessment of air pollutants: a review on spatial heterogeneity and indoor/outdoor/personal exposure to suspended particulate matter, nitrogen dioxide and ozone. *Atmospheric Environment*, 35(6):1–32, 2001.

C Monn, V Carabias, M Junker, R Waeber, M Karrer, and HU Wanner. Small-scale spatial variability of particulate matter < 10 μm (pm10) and nitrogen dioxide. *Atmospheric Environment*, 31(15): 2243–2247, 1997.

JA Mulholland, AJ Butler, JG Wilkinson, AG Russell, and PE Tolbert. Temporal and spatial distributions of ozone in atlanta: Regulatory and epidemiologic implications. *Journal of the Air & Waste Management Association*, 48(5):418–426, 1998.

E Murphy and EA. King. Strategic environmental noise mapping: Methodological issues concerning the implementation of the EU Environmental Noise Directive and their policy implications. *Environment International*, 36(3):290–298, April 2010. ISSN 0160-4120. doi: 10.1016/j.envint.2009.11.006.

E Murphy, HJ Rice, and C Meskell. Environmental noise prediction, noise mapping and GIS integration : the case of inner Dublin, Ireland. In *8th International Transport Noise and Vibration Symposium (June 4-6, 2006, Saint Petersburg; Russia)*. East-European Acoustical Association, 2006. URL `http://irserver.ucd.ie/dspace/handle/10197/3000`.

I Nikolova, S Janssen, K Vrancken, P Vos, V Mishra, and P Berghmans. Size resolved ultrafine particles emission model - a continuous size distribution approach. *Science of the Total Environment*, 409:3492–3499, 2011.

H Pfeiffer, G Baumbach, L Sarachaga-Ruiz, S Kleanthous, O Poulida, and E Beyaz. Neural modelling of the spatial distribution of air pollutants. *Atmospheric Environment*, 43:3289–3297, 2009. doi: 10.1016/j.atmosenv.2008.05.073.

CA Pope III and DW Dockery. Health effects of fine particulate air pollution: lines that connect. *J. Air & Waste Manage. Assoc.*, 56:709–742, 2006.

M Roosli, C Braun-Fahrlander, N Kunzli, L Oglesby, G Theis, M Camenzind, P Mathys, and J Staehelin. Spatial variability of different fractions of particulate matter within an urban environment and between urban and rural sites. *Journal of the Air & Waste Water Management Association*, 50(7):1115–1124, 2000.

Schafer. *The New Soundscape: A handbook for the modern music teacher*. BMI Canada, 1969. ISBN 978-0911320916.

JH Seinfeld and SP Pandis. *Atmospheric Chemistry and Physics: From Air Pollution to Climate Change*. Wiley, Hoboken, New Jersey, second edition, 2006.

XF Shao, M Stein, and J Ching. Statistical comparisons of methods for interpolating the output of a numerical air quality model. *Journal of Statistical Planning and Inference*, 137(7):2277–2293, 2007.

D Shepard. A two-dimensional interpolation function for irregularly spaced data. In *Proceedings, Twenty-third National Conference, Association for Computing Machinery*, pages 517–524, 1968.

JY Son, ML Bell, and JT Lee. Individual exposure to air pollution and lung function in korea spatial analysis using multiple exposure approaches. *Environmental Research*, 110(8):739–749, 2010.

M Stevens. *Community memories for sustainable societies: The case of environmental noise*. PhD thesis, Faculty of Science, Vrije Universiteit Brussel, Brussels, Belgium, June 2012. URL `http://brussense.be/phd-matthias`.

M Tayanc. An assessment of spatial and temporal variation of sulfur dioxide levels over istanbul, turkey. *Environmental Pollution*, 107(1):DOI: 10.1016/S0269–7491(99)00131–1, 2000.

K-T Tsai, M-D Lin, and Y-H Chen. Noise mapping in urban environments: A taiwan study. *Applied Acoustics*, 70(7):964–972, 2009. ISSN 0003-682X. doi: 10.1016/j.apacoust.2008.11.001.

J Viidanoja, M Sillanpaa, J Laakia, VM Kerminen, R Hillamo, P Aarnio, and T Koskentalo. Organic and black carbon in pm2.5 and pm10: 1 year of data from an urban site in helsinki, finland. *Atmospheric Environment*, 36(19):3183–3193, 2002.

YG Wang, PK Hopke, and MJ Utell. Urban-scale spatial-temporal variability of black carbon and winter residential wood combustion particles. *Aerosol and Air Quality Research*, 11(5):473–481, 2011.

D Westerdahl, S Fruin, T Sax, PM Fine, and C Sioutas. Mobile platform measurements of ultrafine particles and associated pollutant concentrations on freeways and residential streets in los angeles. *Atmospheric Environment*, 39(20):3597–3610, 2005.

KW Whitworth, E Symanski, D Lai, and AL Coker. Kriged and modeled ambient air levels of benzene in an urban environment: an exposure assessment study. *Environmental Health*, 10, 2011.

WHO. Guidelines for Community Noise. Technical report, 1999. URL `http://www.who.int/docstore/peh/noise/guidelines2.html`.

WHO Regional Office for Europe. Night noise guidelines for Europe. Technical report, 2009. URL `http://www.euro.who.int/en/what-we-do/health-topics/environmental-health/noise/publications/2009/night-noise-guidelines-for-europe`.

WHO Regional Office for Europe / European Commission Joint Research Centre. Burden of disease from environmental noise. Quantification of healthy life years lost in Europe. Technical report, 2011. URL `http://www.euro.who.int/en/what-we-do/health-topics/environment-and-health/noise/publications/2011/burden-of-disease-from-environmental-noise.-quantification-of-healthy-life-years-lost-in-europe`.

JG Wilson, S Kingham, and AP Sturman. Intraurban variations of pm10 air pollution in christchurch, new zealand: Implications for epidemiological studies. *Science of the Total Environment*, 367: 559–572, 2006.

World Health Organization. Transport, environment and health. WHO regional publications. European series 89, WHO, 2000.

Y Zhu, WC Hinds, S Kim, and C Sioutas. Concentration and size distribution of ultrafine particles near a major highway. *J. Air & Waste Manage. Assoc.*, 52:1032–1042, 2002.